Table 2 Susceptibility loci to the collagen-induced arthritis severity by genome-wide screening in (MRL × DBA/1) F2 mice

		CIA							
		Positive			Negative				
Chromosome	Marker	*D/D*	*D/M*	*M/M*	*D/D*	*D/M*	*M/M*	$\chi 2$	*P* value
5	*D5Mit259*	20	21	5	5	23	18	16.4	0.00027
17	*H-2 (Tnfp)*	19	26	1	4	19	23	31	<0.0001

Mice were genotyped from the 92 phenotypic extremes of the F2 progeny for collagen-induced arthritis (CIA) severity. Values indicate the number of mice. *P*-value in the chi-square test based on a 2 × 3 contingency table with 2 degrees of freedom. Genotypes of mice: *D/D = DBA/DBA* homozygote, *D/M = DBA/MRL* heterozygote, *M/M = MRL/MRL* homozygote.

0.2 weeks in males, indicating that DBA/1 mice were not only susceptible to CIA but also developed CIA with a significantly earlier onset compared to other generations of mice (Table 1). In MDF1 mice, the time of onset was 6.6 ± 1.0 and 5.6 ± 0.7 weeks in females and males, respectively, significantly later than in DBA/1 mice (female $P < 0.01$; male $P < 0.001$). The onset in MDF2 mice (female 4.5 ± 0.3; male 5.3 ± 0.3) was also significantly later than that of DBA/1 mice ($P < 0.001$); however, there was no difference between MDF1 and DMF1 mice. These results suggest that the mode of inheritance of the clinical manifestations of CIA including the incidence, severity, and the time of onset is recessive or incomplete dominant in the genetic contaminant of DBA/1 and MRL mice.

QTL analysis using MDF2 mice

A genome-wide screening of MDF2 mice identified two regions of interest on chromosomes 5 and 17 for CIA severity (Table 2). There was no association between the disease severity and the genotype of the markers, *D1Mit403*, *D2Mit92*, *D7Mit229*, *D15Mit20* and *D19Mit91*, which are previously mapped arthritis susceptibility loci for arthritis of MRL-*Fas*^{lpr} mice (data not shown).[26] Further analysis demonstrated that *H-2*$^{q/q}$ homozygous (median TSI 23) and *H-2*$^{q/k}$ heterozygous (median TSI 18.) mice showed significantly higher severity than *H-2*$^{k/k}$ homozygous mice (median TSI 1, $P < 0.0001$; Fig. 2). In addition, the genotype at *D5Mit259* (chromosome 5, map position 45.0 cM) associated with the TSI ($\chi^2 = 16.4$, $P = 0.00027$) was supported by the QTL analysis, in which the highest LOD score was 6.0 at map position 35 cM between the marker positions *D5Mit183* (29.0 cM) and *D5Mit259* (45 cM) in a dominant mode of inheritance (chromosomal interval 24–56 cM on chromosome 5; Fig. 3). The association between the genotypes at *D5Mit259* and TSI was significant without a male-female difference (data not shown). The screening of extreme progenies revealed that mice that were homozygous and heterozygous for the MRL allele in the region of *D19Mit73* (map position 22.0 cM) developed CIA with an earlier onset than

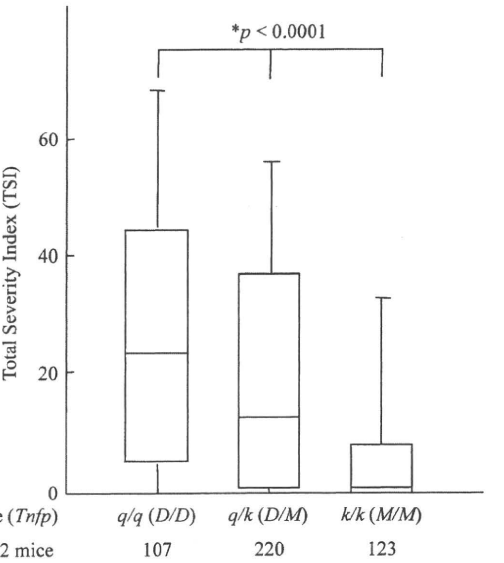

Figure 2 Differences in the total severity index in (MRL × DBA/1) F2 mice at *H-2* locus. The total severity index was grouped according to the genotypes of microsatellite marker *Tnfp*. * *P*-value in the Kruskal-Wallis test. Genotypes of mice: *D/D = DBA/DBA* homozygote, *D/M = DBA/MRL* heterozygote, *M/M = MRL/MRL* homozygote.

parental DBA/1 mice. However, it was not supported by the results from the QTL analysis of all 450 F2 mice (data not shown).

Interaction between *H-2* haplotype and the susceptible locus on chromosome 5

The interlocal interactions between the two susceptibility loci at the *H-2* and *D5Mit183* marker positions were investigated using TSI (Fig. 4). The MDF2 mice with an *H-2* haplotype of *q/q* showed a very high TSI in comparison to the mice with *q/k* and *k/k* independent of the genotypes at *D5Mit183* marker. The differences in the genotype at the *D5mit183* marker remarkably effected the TSI in the presence of *H-2*$^{q/k}$ heterozygous ($P = 0.0018$) or *H-2*$^{k/k}$ homozygous ($P = 0.033$) mice. These results indicate that the DBA/1 mice allele at *D5mit183* marker position independently affects the CIA

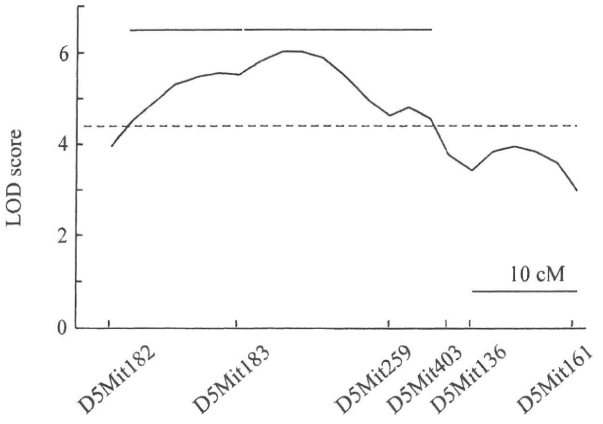

Figure 3 Logarithm of odds (LOD) score plots for quantitative trait loci (QTL) controlling the severity of collagen-induced arthritis in (MRL × DBA/1) F2 mice on chromosomes 5. LOD scores for the presence of a QTL were determined by an interval mapping technique (MAPMAKER/QTL). The most likely position for QTL (confidence interval) is indicated by bar above the plot.

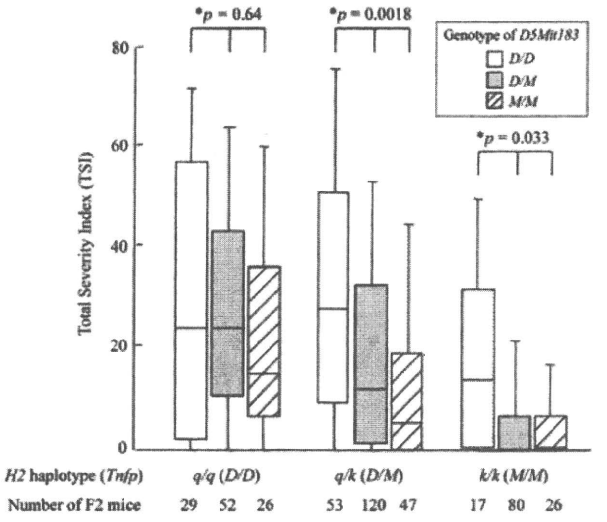

Figure 4 Interaction between 2 collagen-induced arthritis susceptibility loci, *H-2* and *D5Mit183* in (MRL × DBA/1) F2 mice. The total severity index was grouped according to the genotypes at microsatellite marker *Tnfp* and *D5Mit183*, closest to the QTL peak. **P*-values in the Kruskal-Wallis test. Genotypes of mice: *D/D* = *DBA/DBA* homozygote, *D/M* = *DBA/MRL* heterozygote, *M/M* = *MRL/MRL* homozygote.

severity only in the $H\text{-}2^{q/k}$ heterozygote or $H\text{-}2^{q/q}$ homozygous mice, and latently affect the development of arthritis of wild-type DBA/1 mice in the $H\text{-}2^{q/q}$ homozygote.

DISCUSSION

It is important to clarify the genetic basis of diseases in regards to polygenic inheritance, in which polygenes influenced by extrinsic factors are included. Despite the numerous complex traits that have been analyzed in rodents by genome-wide studies, details of the underlying genes are very limited.[33] The cumulative effect of susceptibility genes as a result of genome crossing may be responsible for the diversity of the pathological manifestations of diseases.

CIA is a good model for RA; induced by the immunization with type II collagen extrinsically,[9,10] of which its genetic basis has been well studied, it shows the association with MHC and non-MHC loci.[11–13] While the MRL strain of mice develops spontaneous arthritis associated with an intrinsic factor, the Fas deletion mutant gene *lpr,* this strain seems to be associated with different susceptibility loci from those in CIA, as shown in our previous study.[26] Histopathological features of both arthritic lesions, however, are principally similar, characteristic of granulomatous synovitis with pannus formation to the adjacent bone tissues, suggesting that these lesions develop on a similar pathological sequence, possibly induced by the common polymorphic genes, but not the genes on the downstream activated by the extrinsic and intrinsic factors, type II collagen and the *lpr* gene, respectively. Based on this hypothesis, we examined common and different arthritis susceptible loci induced by these factors.

We found that MRL mice ($H\text{-}2^{k}$) were completely resistant to CIA and reciprocal (MRL × DBA/1) F1 progeny developed CIA with decreased incidence and severity in comparison to DBA/1. The QTL analysis using the F2 generation of DBA/1 and MRL mice identified two susceptibility loci to CIA severity, including $H\text{-}2^{q}$ and the region close to *D5Mit183* on chromosome 5, both of which were derived from the DBA/1 allele. These results were consistent with previous evidence that $H\text{-}2^{k}$ is a resistant haplotype to CIA.[11] The non-MHC locus on chromosome 5 mapped in this study was common to one of the CIA susceptible loci, *Cia13* (*mCia10*, map position; 26–41 cM) which was mapped from the QTL analysis using (BALB/c × DBA/1) F2 mice, and was significantly associated with both disease onset and severity.[18] Numerous susceptibility gene loci have been mapped in other models, including pristane-induced arthritis (PIA) models in rat, and the genes or small intervals responsible for the development of arthritis have been determined by means of recent congenic mapping study.[34,35] The *D5Mit183* locus is orthologous rat chromosome 14 (*D14rat54-D14got1*), involving rat PIA susceptible loci (*Pia6, Pia20*),[36,37] and human chromosome 4 (4p15-p15, 4q11-q12) on which QTL have been identified by independent genome-wide analyses in RA families.[38,39] This indicates that this locus might be common to human RA and other rodent models.

Previous genome-wide screens have identified several loci susceptible to arthritis in MRL mice induced by the Fas^{lpr}, *Paam1* and *Paam2* mapped on chromosome 15 and 19, respectively.[26] Furthermore, the *Amd1* locus on chromosome 10 accelerates the severity and the time of onset in sponta-

neous arthropathy in male DBA/1 mice.[29] However, the association of these loci with CIA was not obvious in this study. This may indicate that the pathologic sequence of arthritis of CIA might use the common allelic loci between two strains MRL and DBA/1 other than the two loci on chromosomes 5 and 17. Otherwise we may have detected more susceptibility loci in this study. The generation of *H-2*$^{a/q}$ congenic MRL mice is now in progress to prove the contribution to the CIA of MRL genetic background.

The arthritis susceptibility locus on the centromeric region of chromosome 5 includes several candidate genes which mediate immunological function, such as *Txk* (*TXK tyrosine kinase*) and *Cd38*. *Txk* is a member of the Tec family tyrosine kinase involved in the T cell activation signal pathway and functions as Th1-specific transcription factor of IFN-γ in co-operation with a factor induced upon T cell receptor signaling.[40,41] The targeted disruption of CD38 accelerates autoimmune diabetes in NOD mice by enhancing autoimmunity in an ADP-ribosyltransferase 2-dependent manner.[42] Further studies to elucidate the polymorphisms and expressions of genes associated with arthritis are therefore needed.

In conclusion, a model was developed which demonstrated that arthritis is controlled not only by MHC gene loci, but also by non-MHC gene loci, and different arthritis models are controlled by a different combination of susceptibility genes with common and different alleles. This indicates that RA is clinically a highly heterogeneous disorder in humans. Future studies using a wide variety of animal models with arthritis will allow for the identification of polymorphic genes and will be helpful to better understanding of the genetic background of RA.

ACKNOWLEDGMENTS

We thank Drs T. Shibata, H. Okumura and LM. Lu for their helpful discussion and M. Terada and N. Arita for their technical assistance. This study was supported with the help of the Integrated Center for Science (INCS), Ehime University.

REFERENCES

1 Harris ED Jr. Rheumatoid arthritis. Pathophysiology and implications for therapy. *N Engl J Med* 1990; **322**: 1277–89.
2 Seldin MF, Amos CI, Ward R, Gregersen PK. The genetics revolution and the assault on rheumatoid arthritis. *Arthritis Rheum* 1999; **42**: 1071–79.
3 Ollier W, Thomson W. Population genetics of rheumatoid arthritis. *Rheum Dis Clin North Am* 1992; **18**: 741–59.
4 Deighton CM, Walker DJ, Griffiths ID, Roberts DF. The contribution of HLA to rheumatoid arthritis. *Clin Genet* 1989; **36**: 178–82.
5 Seidl C, Donner H, Fischer B *et al.* CTLA4 codon 17 dimorphism in patients with rheumatoid arthritis. *Tissue Antigens* 1998; **51**: 62–6.
6 Tokuhiro S, Yamada R, Chang X *et al.* An intronic SNP in a RUNX1 binding site of SLC22A4, encoding an organic cation transporter, is associated with rheumatoid arthritis. *Nat Genet* 2003; **35**: 341–8.
7 Suzuki A, Yamada R, Chang X *et al.* Functional haplotypes of PADI4, encoding citrullinating enzyme peptidylarginine deiminase 4, are associated with rheumatoid arthritis. *Nat Genet* 2003; **34**: 395–402.
8 Begovich AB, Carlton VE, Honigberg LA *et al.* A missense single-nucleotide polymorphism in a gene encoding a protein tyrosine phosphatase (PTPN22) is associated with rheumatoid arthritis. *Am J Hum Genet* 2004; **75**: 330–37.
9 Trentham DE, Townes AS, Kang AH. Autoimmunity to type II collagen an experimental model of arthritis. *J Exp Med* 1977; **146**: 857–68.
10 Courtenay JS, Dallman MJ, Dayan AD, Martin A, Mosedale B. Immunisation against heterologous type II collagen induces arthritis in mice. *Nature* 1980; **283**: 666–68.
11 Wooley PH, Luthra HS, Stuart JM, David CS. Type II collagen-induced arthritis in mice. I. Major histocompatibility complex (I region) linkage and antibody correlates. *J Exp Med* 1981; **154**: 688–700.
12 Wooley PH, Luthra HS, Griffiths MM, Stuart JM, Huse A, David CS. Type II collagen-induced arthritis in mice. IV. Variations in immunogenetic regulation provide evidence for multiple arthritogenic epitopes on the collagen molecule. *J Immunol* 1985; **135**: 2443–51.
13 Couderc J, Gille Perramant MF, Bouthillier Y, Mevel JC. Interactions between H-2 and background genes modulate collagen induced arthritis in high (HI) and low (LI) antibody producer Biozzi mice. *Immunol Lett* 1997; **58**: 43–6.
14 McIndoe RA, Bohlman B, Chi E, Schuster E, Lindhardt M, Hood L. Localization of non-Mhc collagen-induced arthritis susceptibility loci in DBA/1j mice. *Proc Natl Acad Sci USA* 1999; **96**: 2210–14.
15 Jirholt J, Cook A, Emahazion T *et al.* Genetic linkage analysis of collagen-induced arthritis in the mouse. *Eur J Immunol* 1998; **28**: 3321–28.
16 Yang HT, Jirholt J, Svensson L *et al.* Identification of genes controlling collagen-induced arthritis in mice: Striking homology with susceptibility loci previously identified in the rat. *J Immunol* 1999; **163**: 2916–21.
17 Johansson AC, Sundler M, Kjellen P *et al.* Genetic control of collagen-induced arthritis in a cross with NOD and C57BL/10 mice is dependent on gene regions encoding complement factor 5 and FcgammaRIIb and is not associated with loci controlling diabetes. *Eur J Immunol* 2001; **31**: 1847–56.
18 Adarichev VA, Valdez JC, Bardos T, Finnegan A, Mikecz K, Glant TT. Combined autoimmune models of arthritis reveal shared and independent qualitative (binary) and quantitative trait loci. *J Immunol* 2003; **170**: 2283–92.
19 Johannesson M, Karlsson J, Wernhoff P *et al.* Identification of epistasis through a partial advanced intercross reveals three arthritis loci within the Cia5 QTL in mice. *Genes Immun* 2005; **6**: 175–85.
20 Bauer K, Yu X, Wernhoff P, Koczan D, Thiesen HJ, Ibrahim SM. Identification of new quantitative trait loci in mice with collagen-induced arthritis. *Arthritis Rheum* 2004; **50**: 3721–28.
21 Karlsson J, Johannesson M, Lindvall T, Wernhoff P, Holmdahl R, Andersson A. Genetic interactions in Eae2 control collagen-induced arthritis and the CD4+/CD8+ T cell ratio. *J Immunol* 2005; **174**: 533–41.
22 Murphy ED, Roths JB. Autoimmunity and lymphoproliferation: Induction by mutant gene lpr, and acceleration by a male-associated factor in strain BXSB mice. In: Rose NR, Bigazzi PE,

Warner NL, eds. *Genetic Control of Autoimmune Disease.* New York: Elsevier North Holland, 1978; 207–20.
23 Izui S, Eisenberg RA. Circulating anti-DNA-rheumatoid factor complexes in MRL/1 mice. *Clin Immunol Immunopathol* 1980; **15**: 536–51.
24 Hang L, Theofilopoulos AN, Dixon FJ. A spontaneous rheumatoid arthritis-like disease in MRL/l mice. *J Exp Med* 1982; **155**: 1690–701.
25 Nardella FA, Teller DC, Izui S, Mannik M. Self-associating IgG rheumatoid factors in MRL/l autoimmune mice. *Arthritis Rheum* 1984; **27**: 1165–73.
26 Kamogawa J, Terada M, Mizuki S *et al.* Arthritis in MRL/lpr mice is under the control of multiple gene loci with an allelic combination derived from the original inbred strains. *Arthritis Rheum* 2002; **46**: 1067–74.
27 Jongeneel CV, Acha Orbea H, Blankenstein T. A polymorphic microsatellite in the tumor necrosis factor alpha promoter identifies an allele unique to the NZW mouse strain. *J Exp Med* 1990; **171**: 2141–46.
28 Lander ES, Botstein D. Mapping mendelian factors underlying quantitative traits using RFLP linkage maps. *Genet* 1989; **121**: 185–99.
29 Oishi H, Miyazaki T, Mizuki S *et al.* Accelerating effect of an MRL gene locus on the severity and onset of arthropathy in DBA/1 mice. *Arthritis Rheum* 2005; **52**: 959–66.
30 Lander ES, Green P, Abrahamson J *et al.* MAPMAKER: An interactive computer package for constructing primary genetic linkage maps of experimental and natural populations. *Genomics* 1987; **1**: 174–81.
31 Paterson AH, Lander ES, Hewitt JD, Peterson S, Lincoln SE, Tanksley SD. Resolution of quantitative traits into Mendelian factors by using a complete linkage map of restriction fragment length polymorphisms. *Nature* 1988; **335**: 721–26.
32 Lander E, Kruglyak L. Genetic dissection of complex traits: Guidelines for interpreting and reporting linkage results. *Nat Genet* 1995; **11**: 241–47.
33 Glazier AM, Nadeau JH, Aitman TJ. Finding genes that underlie complex traits. *Science* 2002; **298**: 2345–49.
34 Olofsson P, Holmberg J, Tordsson J, Lu S, Akerstrom B, Holmdahl R. Positional identification of Ncf1 as a gene that regulates arthritis severity in rats. *Nat Genet* 2003; **33**: 25–32.
35 Laragione T, Yarlett NC, Brenner M *et al.* The arthritis severity quantitative trait loci Cia4 and Cia6 regulate neutrophil migration into inflammatory sites and levels of TNF-alpha and nitric oxide. *J Immunol* 2007; **178**: 2344–51.
36 Vingsbo Lundberg C, Nordquist N, Olofsson P *et al.* Genetic control of arthritis onset, severity and chronicity in a model for rheumatoid arthritis in rats. *Nat Genet* 1998; **20**: 401–4.
37 Wester L, Olofsson P, Ibrahim SM, Holmdahl R. Chronicity of pristane-induced arthritis in rats is controlled by genes on chromosome 14. *J Autoimmun* 2003; **21**: 305–13.
38 Jawaheer D, Seldin MF, Amos CI *et al.* A genomewide screen in multiplex rheumatoid arthritis families suggests genetic overlap with other autoimmune diseases. *Am J Hum Genet* 2001; **68**: 927–36.
39 Osorio Y, Fortea J, Bukulmez H *et al.* Dense genome-wide linkage analysis of rheumatoid arthritis, including covariates. *Arthritis Rheum* 2004; **50**: 2757–65.
40 Schaeffer EM, Debnath J, Yap G *et al.* Requirement for Tec kinases Rlk and Itk in T cell receptor signaling and immunity. *Science* 1999; **284**: 638–41.
41 Takeba Y, Nagafuchi H, Takeno M, Kashiwakura J, Suzuki N. Txk, a member of nonreceptor tyrosine kinase of Tec family, acts as a Th1 cell-specific transcription factor and regulates IFN-gamma gene transcription. *J Immunol* 2002; **168**: 2365–70.
42 Chen J, Chen YG, Reifsnyder PC *et al.* Targeted disruption of CD38 accelerates autoimmune diabetes in NOD/Lt mice by enhancing autoimmunity in an ADP-ribosyltransferase 2-dependent fashion. *J Immunol* 2006; **176**: 4590–99.

Lack of lacto/neolacto-glycolipids enhances the formation of glycolipid-enriched microdomains, facilitating B cell activation

Akira Togayachi[a], Yuko Kozono[a], Yuzuru Ikehara[a], Hiromi Ito[a], Nami Suzuki[a], Yuki Tsunoda[a], Sumie Abe[a], Takashi Sato[a], Kyoko Nakamura[b], Minoru Suzuki[b], Hatsumi M. Goda[c], Makoto Ito[c], Takashi Kudo[d], Satoru Takahashi[d], and Hisashi Narimatsu[a,1]

[a]Research Center for Medical Glycoscience, National Institute of Advanced Industrial Science and Technology, Central-2 OSL, 1-1-1 Umezono, Tsukuba, Ibaraki 305-8568, Japan; [b]Sphingolipid Expression Laboratory, Supra-Biomolecular System Research Group, RIKEN Frontier Research System, 2-1 Hirosawa, Wako, Saitama 351-0198, Japan; [c]Department of Bioscience and Biotechnology, Graduate School of Bioresource and Bioenvironmental Sciences, Kyushu University, 6-10-1 Hakozaki, Higashi-ku, Fukuoka 812-8581, Japan; and [d]Department of Anatomy and Embryology, Graduate School of Comprehensive Human Sciences, University of Tsukuba, 1-1-1 Tennodai, Tsukuba, Ibaraki 305-8575, Japan

Edited* by Senitiroh Hakomori, Pacific Northwest Research Institute, Seattle, WA, and approved May 10, 2010 (received for review December 16, 2009)

In a previous study, we demonstrated that β1,3-*N*-acetylglucosaminyltransferase 5 (*B3gnt5*) is a lactotriaosylceramide (Lc_3Cer) synthase that synthesizes a precursor structure for lacto/neolacto-series glycosphingolipids (GSLs) in in vitro experiments. Here, we generated *B3gnt5*-deficient (*B3gnt5*$^{-/-}$) mice to investigate the in vivo biological functions of lacto/neolacto-series GSLs. In biochemical analyses, lacto/neolacto-series GSLs were confirmed to be absent and no Lc_3Cer synthase activity was detected in the tissues of these mice. These results demonstrate that β3GnT5 is the sole enzyme synthesizing Lc_3Cer in vivo. Ganglioside GM1, known as a glycosphingolipid-enriched microdomain (GEM) marker, was found to be upregulated in *B3gnt5*$^{-/-}$ B cells by flow cytometry and fluorescence microscopy. However, no difference in the amount of GM1 was observed by TLC-immunoblotting analysis. The GEM-stained puncta on the surface of *B3gnt5*$^{-/-}$ resting B cells were brighter and larger than those of WT cells. These results suggest that structural alteration of GEM occurs in *B3gnt5*$^{-/-}$ B cells. We next examined whether BCR signaling-related proteins, such as BCR, CD19, and the signaling molecule Lyn, had moved into or out of the GEM fraction. In *B3gnt5*$^{-/-}$ B cells, these molecules were enriched in the GEM fraction or adjacent fraction. Moreover, *B3gnt5*$^{-/-}$ B cells were more sensitive to the induction of intracellular phosphorylation signals on BCR stimulation and proliferated more vigorously than WT B cells. Together, these results suggest that lacto/neolacto-series GSLs play an important role in clustering of GEMs and tether-specific proteins, such as BCR, CD19, and related signaling molecules to the GEMs.

β1,3-*N*-acetylglucosaminyltransferase | glycosyltransferase | polylactosamine | glycosphingolipid | B cell receptor

Almost all organisms possess lipids and proteins to which a broad range of carbohydrate chains are linked. Some carbohydrate structures are known to participate in vital processes, such as the molecules responsible for cell–cell, receptor–ligand, and carbohydrate–carbohydrate interactions. It is known that glycosphingolipids (GSLs) have an important role in biological functions. In mammals, GSLs can be classified into several major classes, such as globo-, isoglobo-, ganglio-, and lacto/neolacto-series GSLs and others (Fig. S1). Gangliosides that contain one or more sialic acids on their carbohydrate chains modulate the responsiveness of signaling molecules and cell surface receptors (1). Some functional carbohydrate antigens, such as blood group Lewis antigens and the HNK-1 antigen, are carried on lacto/neolacto-series GSLs. During the development of hematopoietic cells, expression of HNK-1 (CD57) and Lewis-related antigens on lacto/neolacto-series GSLs is spatially and temporally regulated; the expression of such GSLs is also dramatically changed during the immune response (2).

Membrane microdomains are cholesterol- and GSL-rich components of the plasma membrane, also known as glycosphingolipid-enriched microdomains (GEMs), glycosphingolipid-signaling domains, lipid rafts, detergent-resistant membrane structures (DRMs), or detergent-insoluble glycolipid-enriched complex (3–5). General/classic lipid rafts, referred to here as GEMs, serve as platforms for different mechanisms of cell signaling. GEMs contain other sphingolipids, cholesterol, GPI-anchored proteins, many receptor molecules, and selected signaling molecules. GSLs are major components of GEMs. GSLs in microdomains are involved in various biological functions, such as signal transduction, toxin and infection receptors for bacteria and viruses (6), cell adhesion (5, 7), and cell growth modulation (8). It is thought that the most probable function exerted by GSLs in microdomains is to concentrate proteins that play a role in transmembrane signaling events and their regulated activation (9). GEMs also contain many important molecules, including immunoreceptors, such as the B cell receptor (BCR), T cell receptor (TCR), CD4, and CD8 among others, as well as cellular signaling molecules (10–14). It is known that GPI-anchored glycoproteins, such as CD48, CD59, and others, are also localized within GEMs. Recent studies have also shown the importance of GEM formation in cell differentiation and the acquired immune response among other processes. In T cells, clustering of GEMs regulates sustained TCR signaling because this process maintains engagement of the TCR with costimulators, such as CD28 and GPI-anchored glycoproteins, leading to partitioning within GEMs and resulting in exclusion of large highly glycosylated proteins, such as CD43 and CD45 (15). For facilitating sustained TCR signal transduction, TCR localization within GEMs results in high local concentrations of TCR signal-related molecules, such as protein tyrosine kinases and signal transducers, and the exclusion of CD45 phosphatase activity, which negatively regulates TCR signaling.

β1,3-*N*-acetylglucosaminyltransferases (β3GnTs) transfer an *N*-acetylglucosamine (GlcNAc) from UDP-GlcNAc to Gal on the nonreducing end of the carbohydrate chain with a β1,3-linkage. At present, eight members of the human β3GnT family have been cloned and characterized (16). In a previous study (17), β3GnT5 was cloned as lactotriaosylceramide (Lc_3Cer) synthase and characterized as a key enzyme for the biosynthesis of lacto/neolacto-series GSLs (17, 18). *B3gnt2* (*β3GnT2*) mRNA is ubiquitously

Author contributions: A.T., Y.K., Y.I., H.I., T.S., T.K., S.T., and H.N. designed research; A.T., Y.K., Y.I., H.I., N.S., Y.T., S.A., K.N., M.S., H.M.G., M.I., T.K., and S.T. performed research; K.N., M.S., H.M.G., and M.I. contributed new reagents/analytic tools; A.T., Y.K., Y.I., H.I., N.S., Y.T., S.A., T.S., K.N., M.S., H.M.G., M.I., T.K., S.T., and H.N. analyzed data; and A.T. and H.N. wrote the paper.

The authors declare no conflict of interest.

*This Direct Submission article had a prearranged editor.

Data deposition: The sequence reported in this paper has been deposited in the GenBank database (accession no. AB045278).

[1]To whom correspondence should be addressed. E-mail: h.narimatsu@aist.go.jp.

This article contains supporting information online at www.pnas.org/lookup/suppl/doi:10.1073/pnas.0914298107/-/DCSupplemental.

expressed in mouse tissues, and thus also in B cells, T cells, and other immune cells. The previous study demonstrated that *B3gnt2*$^{-/-}$ B and T cells, which lack polylactosamine (PLN) on the *N*-glycans of their glycoproteins, showed hyperactivation following BCR or TCR/CD28 stimulation (19). Thus, PLN chains on glycoproteins have an important role in determining thresholds for in vitro immunocyte activation. On the other hand, we and other groups have observed that the expression of *B3gnt5* mRNA is limited mainly to B cells (Fig. S1). We are also interested in the functions of PLN chains not only on glycoproteins but on GSLs in B cells.

It has been reported that disruption of the *B3gnt5* gene leads to preimplantation lethality; therefore, no individuals homozygous for *B3gnt5*-null alleles are viable (20). However, we have succeeded in generating *B3gnt5*-deficient mice by a different approach, for example, by using a different ES cell clone and genomic construction (targeting vector). The *B3gnt5*$^{-/-}$ mice generated in this study were viable and fertile and showed normal growth, although they were *B3gnt5*-null in all tissues tested. Thus, this study on gene-disrupted mice lacks lacto/neolacto-series GSLs. We found that abnormal formation of GEMs was significantly increased in *B3gnt5*$^{-/-}$ mice. This observation prompted us to investigate whether the mice show immunological disorders of B cells and how lacto/neolacto-series GSLs are involved in BCR/CD19 signaling.

Results

Generation of *B3gnt5*$^{-/-}$ Mice. Quantitative real-time RT-PCR analysis confirmed that *B3gnt5* mRNA expression was present at a high level in immune organs and/or cells (Fig. S1). To analyze whether disorders of the immune system would occur in its absence, we generated *B3gnt5*-deficient mice.

To confirm the generation of *B3gnt5*-deficient mice, we analyzed expression of the *B3gnt5* gene and lactotriaosylceramide (Lc_3Cer)-synthesizing activity in the tissues of WT and *B3gnt5*$^{-/-}$ mice. Previously, we reported that the HL-60 cell line expressed abundant *B3gnt5* transcripts, whereas the Jurkat cell line did not (17). In Fig. 1, tissue homogenates of WT mice showed apparent activity of Lc_3Cer synthase in all organs except the cerebrum. This is consistent with a previous report by others in which the adult cerebral cortex was found to express little or no *B3gnt5* transcript. In contrast, the adult cerebellum expresses *B3gnt5* transcripts at a comparatively high level in Purkinje cells (18). Tissue homogenates of *B3gnt5*$^{-/-}$ mice exhibited no Lc_3Cer-synthesizing activity. These results indicate that there is no other glycosyltransferase with Lc_3Cer-synthesizing activity.

Glycan Structure of GSLs Extracted from Tissues of WT and *B3gnt5*-Deficient Mice. We performed TLC-immunoblotting using anti-GlcNAc Ab (kindly provided by Minoru Suzuki, RIKEN, Saitama, Japan) on GSLs from the cerebellum. Orcinol staining revealed no differences in the patterns of GSLs (Fig. S2). This is probably attributable to the low content of lacto/neolacto-series GSLs as compared with gangliosides. However, the immunoblotting results shown in Fig. S2 clearly demonstrated that Lc_3Cer (amino-CTH) was absent in the *B3gnt5*$^{-/-}$ cerebellum. On the other hand, we could not detect the signal for Lc_3Cer on TLC (-immunoblotting) analysis of spleen, probably because the amount of Lc_3Cer was too low in total GSLs. Orcinol staining again showed no difference between WT and *B3gnt5*$^{-/-}$ mice in acidic GSLs from spleen (Fig. S2). By immunostaining the acid fraction of GSLs treated with sialidase, at least three positive bands were detected in WT spleen using the 1B2-1B7 mAb (Fig. S2). These bands entirely disappeared in *B3gnt5*$^{-/-}$ mice. It is known that mAb 1B2-1B7 reacts with neolactotetraosylceramide (nLc_4Cer), nLc_6Cer, and other glycolipids having LacNAc units at the nonreducing end of their carbohydrate chains.

As seen from the results of MS analysis (Fig. 1 and Fig. S2), we confirmed the loss of elongated GSLs on Lc_3Cer in *B3gnt5*$^{-/-}$ B cells. Signals of nos. 7 and 16 were absent in *B3gnt5*$^{-/-}$ mice, although they were present in WT B cells. No. 7 was identified as

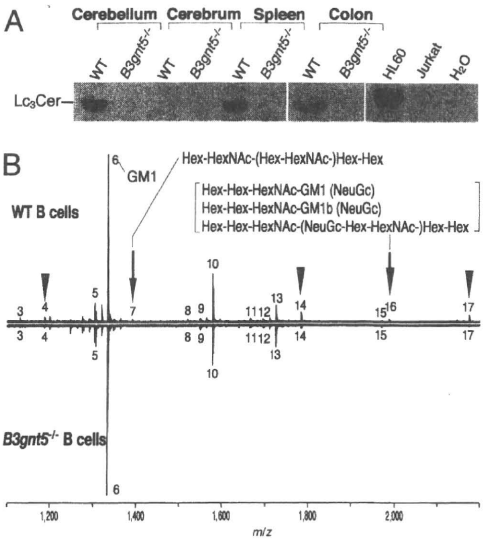

Fig. 1. Confirmation of Lc_3Cer synthase activity in *B3gnt5*$^{-/-}$ mice and MS analysis of the glycans derived from GSLs of mouse B cells. (*A*) Homogenates (100 μg of protein) of mouse tissues were used to assay Lc_3Cer synthase activity. The products were separated on a high-performance twin-layer chromatography (HPTLC) plate with a solvent system of chloroform/methanol/0.2% $CaCl_2$ (60:35:8 vol/vol/vol). The intensities of the radioactive bands were measured with a FLA3000 Image Analyzer, (Fujifilm, Tokyo). HL-60, which has Lc_3Cer synthase activity, and Jurkat, which does not, were used as positive and negative controls, respectively. Lc_3Cer synthase assays were performed on two TLC plates, with positive and negative control on each plate. This figure was prepared from the results of two TLC plates to demonstrate Lc_3Cer synthase activity in cerebellum, spleen, and colon between WT and *B3gnt5*$^{-/-}$ mice. (*B*) MS spectra of the glycans derived from GSLs of mouse B cells. Arrows indicate glycan signals that are absent from GSLs of *B3gnt5*$^{-/-}$ B cells. Arrowheads indicate glycan signals that are decreased in GSLs of *B3gnt5*$^{-/-}$ B cells. Table S1 summarizes the results of the assigned GSL-derived glycan structures of mouse B cells. Detailed methods for MS of glycans derived from GSLs are described in Fig. S2.

Galβ1-4GlcNAcβ1-3(Galβ1-4GlcNAcβ1-6)Galβ1-4Glc, which is one of the lacto/neolacto-series GSL structures, using the method described in *SI Experimental Procedures and Results*. The *m/z* (1,987.147) of no. 16 indicates three candidates that are possibly ganglio-series glycolipids or lacto/neolacto-series GSLs, as listed in Table S1. In in vitro recombinant β3GnT5, enzyme acts on ganglio-series GSLs, including GA1, GM1 (GM1a), and GD1b, as an acceptor substrate (18). Therefore, this is likely to be one of the lacto/neolacto-series GSLs having a Hex-Hex-*N*-acetylhexosamine (HexNAc)-[sialic acid (NeuGc)-Hex-HexNAc] Hex-Hex structure and/or one of the ganglio-series GSLs having a Hex-Hex-HexNAc-GM1a structure, because it was absent in the B cells of *B3gnt5*$^{-/-}$ mice. The signals of nos. 4, 14, and 17 (Fig. 1*B* and Fig. S2) significantly decreased in *B3gnt5*$^{-/-}$ B cells. These molecular masses correspond to both ganglio-series and lacto/neolacto-series GSLs, as listed in Table S1. A mixture of both ganglio-series and lacto/neolacto-series GSLs may be contained in these samples, and the lack of lacto/neolacto-series and/or minor ganglio-series GSLs in *B3gnt5*$^{-/-}$ B cells may reflect this.

Flow Cytometry and Immunoblot Analyses of PLN Using *Lycopersicon esculentum* Lectin. Our previous study indicated that of the four members of the β3GnTs, β3GnT2 exhibits the strongest PLN synthetic ability in vitro and that β3GnT5 shows lower activity, ~30% of that of β3GnT2 (17). To examine whether PLN on glycoproteins is affected in *B3gnt5*$^{-/-}$ mice, flow cytometry (FCM) analysis of splenocytes was performed using *Lycopersicon esculentum* (LEL) lectin. This lectin binds to PLN chains having at least three LacNAc repeats. By FCM, no difference between

WT and *B3gnt5*$^{-/-}$ splenocytes and B cells in LEL staining at the cell surface was observed (Fig. S3). As seen in Fig. S3, blotting analysis using LEL showed strong signals for both WT and *B3gnt5*$^{-/-}$ splenocytes without any significant difference of intensity as compared with *B3gnt2*$^{-/-}$ splenocytes. This suggests that β3GnT5 is not involved in the expression of PLN chains on glycoproteins.

FCM Analysis of Hematocytes in *B3gnt5*-Deficient Mice. To investigate whether hematocytes manifest aberrant cell distribution or development in *B3gnt5*$^{-/-}$ mice, we analyzed the expression of a series of CD antigens on the cell surface of peripheral blood and splenic cells using FCM. The antigens investigated were the same as those described in a previous study (19). No significant disturbance in the ratios of cell populations, such as T cells, B cells, monocytes, or granulocytes, was observed. However, we documented a marginal increase in Ab levels in intact mouse serum; the levels of total IgG, IgG_{2a}, and IgG_{2b} were increased in *B3gnt5*$^{-/-}$ mice as compared with WT mice (Fig. S4). Lacto/neolacto-GSLs are known to be localized in GEMs on the cell surface. However, some antibodies that bind to lacto/neolacto-GSLs, such as the anti-LacNAc mAb 1B2-1B7, are known to cross-react with carbohydrate antigens on glycoproteins. Therefore, we investigated GSL antigens on the cell surface (i.e., GM1, GM3, Gb3, others) as GEM markers. In a series of FCM analysis, we were interested to observe that the intensity of GM1 staining with Ab or cholera toxin B subunit (CT-B) was significantly increased in the B cells of *B3gnt5*$^{-/-}$ mice as compared with WT mice (Fig. 2). GM1 levels were increased on splenic B cells (Fig. 2, gate: $CD19^+$ cells) of *B3gnt5*$^{-/-}$ mice [mean fluorescence intensity (MFI) of ~1,431] as compared with WT mice (MFI of ~625).

BCR and CD19 antigens on the B cell surface were not different in WT and *B3gnt5*$^{-/-}$ mice. There was also no difference in the level of expression of these molecules in WT or *B3gnt5*$^{-/-}$ mice, as assessed by Western blotting (Fig. S5). Because it is known that many GPI-anchored proteins are localized in GEMs, we examined the expression profiles of other GPI-anchored proteins, such as CD48. However, we found no differences between WT and *B3gnt5*$^{-/-}$ mice in any expression profiles. In contrast to these findings with B cells, T cells did not manifest any differences in GM1 expression detected by CT-B. This may be interpreted in relation to their initially low expression of *B3gnt5* transcripts.

Microscopic Analysis of GEMs in B Cells. We observed GEM formation on the cell surface using cholera toxin as a probe, because it is known that CT-B binds to GM1. CT-B and various GPI-anchored proteins have been defined and identified previously as components of GEMs. CT-B staining of the cell surface showed a punctate pattern by fluorescence microscopy (Fig. 3). This pattern was identical to that reported in previous studies. In the present study, the puncta on the surface of *B3gnt5*$^{-/-}$ resting B cells were much brighter and larger and their number was significantly increased as compared with WT. These CT-B staining levels for the puncta of *B3gnt5*$^{-/-}$ resting cells were almost as high as for stimulated WT B cells (Fig. 3). Thus, the B cells of *B3gnt5*$^{-/-}$ mice may be easier to activate; furthermore, the staining levels of puncta were increased even more in stimulated B cells of *B3gnt5*$^{-/-}$ mice as compared with stimulated WT cells.

Because GM1 staining on FCM was up-regulated, we examined six transcripts for glycosyltransferase genes involved in the synthesis of GM1 in resting B cells from WT and *B3gnt5*$^{-/-}$ mice. By the comparative PCR method using real-time PCR (Fig. S6), there were no significant differences between the B cells of WT and *B3gnt5*$^{-/-}$ mice in the levels of these six transcripts. No expression of *B3gnt5* mRNA in resting B cells of *B3gnt5*$^{-/-}$ mice could be confirmed. In addition, the pattern of MS spectra indicated no marked change in the amount of GM1, with the exception of the decreased peak intensity related to lacto/neolacto-series GSLs. (Fig. 1 and Fig. S2). However, MS analysis and orcinol staining of GSLs on TLC (Fig. S6) are, in general, poorly

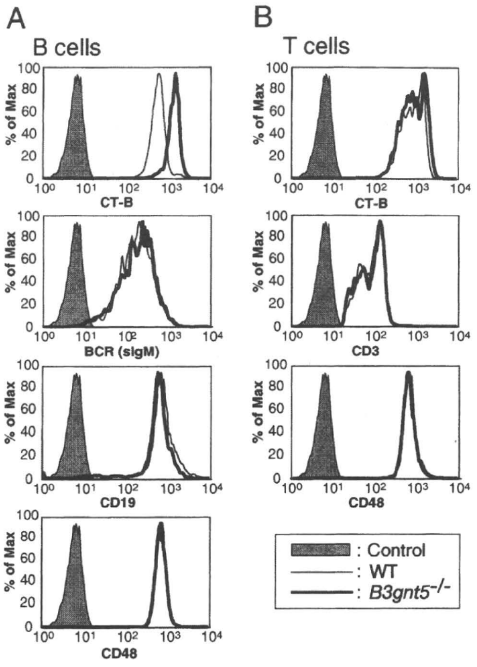

Fig. 2. Up-regulation of CT-B staining as a GEM marker but no alteration of surface protein expression on B cells. FCM analysis of GEMs and surface proteins on splenic B cells (*A*) and T cells (*B*). The expression on the splenocyte cell surface was analyzed by FCM using FITC-conjugated CT-B, anti-CD3ε, anti-BCR (sIgM), anti-CD48 Abs, and phycoerythrin (PE)-conjugated anti-CD19. Results are shown as histograms of fluorescence intensity. The shaded peak in each panel represents the negative control. Max, maximum.

quantitative. Therefore, the total amount of GM1 in B cells was determined by TLC-immunoblotting using HRP-conjugated CT-B. Total amounts of GM1 did not differ between WT and *B3gnt5*$^{-/-}$ mice (Fig. S6).

Distribution Analysis of GEM Proteins. As reported in the previous studies, we observed in this study that BCR, CD19, and Lyn of B cells were colocalized in low-density membrane fraction GEMs (Fig. 4, designated fractions 1–4) prepared in medium containing 1% Triton X-100 and separated by sucrose density gradient centrifugation. We analyzed the behavior of BCR transduction-related proteins in GEMs after stimulation with anti-BCR Ab and anti-CD19 Ab cross-linking (Fig. 4). Western blotting showed that the BCR and CD19 antigens from B cells of *B3gnt5*$^{-/-}$ mice were markedly increased in the GEM fraction, as compared with WT mice. In addition, larger amounts of Lyn kinases were located in the GEM fraction in *B3gnt5*$^{-/-}$ B cells. On the other hand, we determined that not only cross-linking of BCR together with CD19 but cross-linking of CD19 alone resulted in abnormalities in the GEM structure. This suggests that GEM-related molecules, such as BCR, CD19, and Lyn, show increased motility into GEM (fractions 1–4; Fig. S7). These results indicated that *B3gnt5*$^{-/-}$ B cells might be in a state in which they could be more easily activated by external stimuli as compared with WT B cells. We therefore propose that GEM abnormalities are present in *B3gnt5*$^{-/-}$ B cells.

Phosphorylation Signals Under BCR Stimulation Are Increased in B Cells of *B3gnt5*-Deficient Mice. Many kinases have been reported to play important roles in signal transduction following BCR stimulation. To analyze the alteration of BCR downstream signals after anti-BCR cross-linking, we examined phosphorylation patterns in B cells of WT and *B3gnt5*$^{-/-}$ mice. Western blotting with the Ab 4G10, specific for phosphotyrosine, yielded multiple

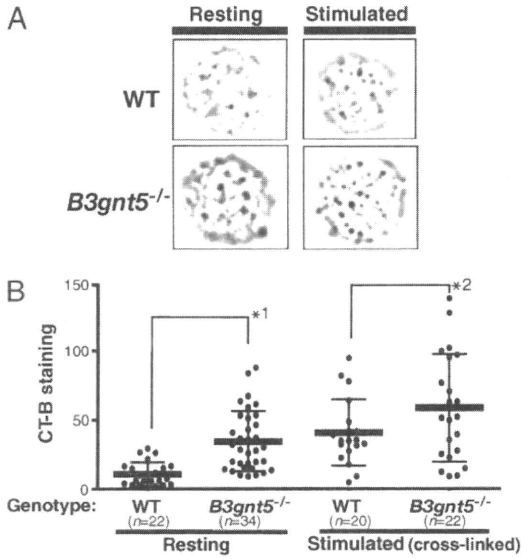

Fig. 3. Fluorescence microscopy of GEMs on the cell surface. (*A*) Fluorescence microscopy showed a CT-B–induced punctate pattern indicating GEM structures on the B cell surface. Resting or stimulated isolated B cells were stained with FITC-conjugated CT-B. The results shown are representative of several independent experiments revealing markedly stronger staining of *B3gnt5*$^{-/-}$ than WT B cells. (*B*) Fluorescence intensity of positive signals for each CT-B–stained punctate region was analyzed by means of a BZ-Analyzer (KEYENCE). The total value of the positive signals on each cell surface was measured. Statistical analysis of the difference between WT and *B3gnt5*$^{-/-}$ B cells, with or without stimulation, was performed using one-way ANOVA and Tukey testing by means of PRISM4 software. Data are given as each cell type's mean (bold line) and SD. *1, $P < 0.01$; *2, $P < 0.01$.

bands (Fig. 5). Immunoblotting with Ab 4G10 showed that tyrosine phosphorylation of multiple proteins in *B3gnt5*$^{-/-}$ B cells was dramatically increased as compared with WT mice.

Enhanced Response of Stimulated *B3gnt5*-Deficient B Cells. BCR and CD19 are major immune receptors and costimulatory molecules, respectively, for B cell activation (21). Because the behavior of these molecules in GEMs was different between WT and *B3gnt5*$^{-/-}$ B cells, we examined the impact of lacto/neolacto-GSL deficiency on B cell proliferation. Resting B cells were stimulated with anti-BCR (anti-IgM) and assessed for proliferation after 2 d. A greater proliferation of *B3gnt5*$^{-/-}$ than WT splenic B cells was observed with low concentrations of anti-BCR (Fig. 5). These results indicate that the lack of PLN in GSLs of B cells lowers the cellular threshold for proliferation triggered by BCR stimulation. In addition, we examined the in vivo response to the T-independent type II antigen [TI-II antigen, trinitrophenol (TNP)-Ficoll]. The specific Ab response to TNP was slightly up-regulated in *B3gnt5*$^{-/-}$ mice (Fig. 5*C*). The levels of IgM production were up-regulated at an early stage of the response in *B3gnt5*$^{-/-}$ mice as compared with WT mice. However, 14 d after immunization, differences between WT and *B3gnt5*$^{-/-}$ mice were no longer apparent in the levels of TNP-specific Ab produced.

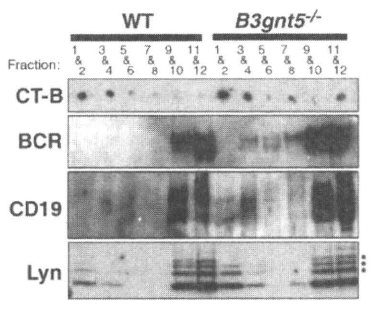

Fig. 4. Distribution of BCR, CD19, and Lyn in GEMs separated into fractions by sucrose density gradient centrifugation. B cells stimulated with anti-BCR and anti-CD19 Abs were lysed with 1% Triton X-100 solubilization buffer. After sucrose gradient centrifugation, fractions were collected from the top of gradient. Then, every second fraction was combined starting from the top fraction. GM1, a GEM marker, was detected using HRP-conjugated CT-B as shown. After fractionation, immunoprecipitation of BCR and CD19 was performed using anti-BCR and anti-CD19 Abs, respectively. BCR (sIgM) and CD19 proteins in *B3gnt5*$^{-/-}$ B cells were up-regulated in the GEM fraction (fractions 1–4). Lyn proteins were also up-regulated in the GEM fraction of *B3gnt5*$^{-/-}$ B cells. The results shown are representative of several independent experiments. *Nonspecific bands.

Discussion

The results of previous studies had strongly indicated that β3GnT5 was the most feasible candidate for the Lc_3Cer synthase (17, 18). We had also determined that mouse B cells expressed abundant *B3gnt5* transcripts and possessed Lc_3Cer synthase activity. To approach the question of the significance of lacto/neolacto-series GSLs in biological function, we generated *B3gnt5*$^{-/-}$ mice. In the present study, we confirmed that Lc_3Cer synthase activity was undetectable in any of the tissue homogenates of *B3gnt5*$^{-/-}$ mice examined. These results indicate that Lc_3Cer synthase is the sole enzyme responsible for the extension of PLN chains on lacto/neolacto-series GSLs.

Lacto/neolacto-series GSLs contain sialic acid or sulfate, resulting in sialylparagloboside, sulfoglucuronylglycolipid, and other

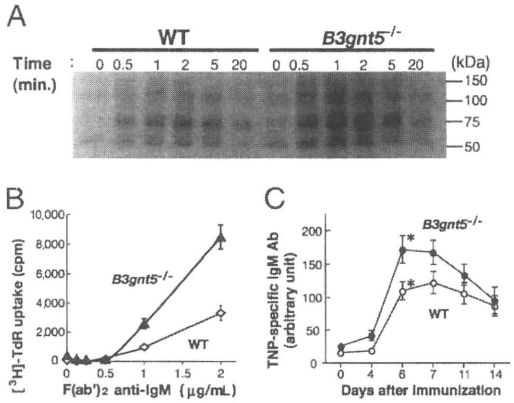

Fig. 5. Analysis of phosphorylation status and enhanced response to BCR cross-linking in resting B cells. (*A*) Resting B cells from spleen were stimulated by cross-linking anti-BCR Ab for the indicated time. The same volume of lysates was added to each lane. Phosphorylated proteins were analyzed by immunoblots using anti-phospho-Tyr mAb (4G10). *B3gnt5*$^{-/-}$ B cells exhibited significantly up-regulated phosphorylation signals. (*B*) Resting B cells from *B3gnt5*$^{-/-}$ mice show enhanced responses to BCR-mediated stimulation. Resting B cells were cultured with the indicated dose of $F(ab')_2$ anti-IgM. Proliferative responses are given as $[^3H]$-thymidine (TdR) incorporation for the final 6 h of the 42-h culture period. Each assay was performed in triplicate, and all data are representative of three experiments. Open circles indicate WT mice, and closed triangles indicate *B3gnt5*$^{-/-}$ mice. (*C*) Response to TI-II antigen. Mice were immunized i.p. with 25 μg of TNP-Ficoll in PBS at day 0. Sera were collected sequentially from the eye socket and tested at a 1:100 dilution. The levels of TNP-specific IgM Ab in sera were determined by ELISA. Representative data were obtained for five (WT) and six (*B3gnt5*$^{-/-}$) mice, respectively. Open circles indicate WT mice, and closed circles indicate *B3gnt5*$^{-/-}$ mice. Statistical analysis of the difference between WT and *B3gnt5*$^{-/-}$ B cells with days after stimulation was performed by two-way ANOVA using PRISM4 software. The levels of IgM in serum are presented as mean (symbols) ± SE. *$P < 0.05$.

similar derivatives. Mouse lymphocytes contain globo-series GSLs (Gb3 and Gb4) and ganglio-series GSL (GM3) (22), but it was not known whether they possessed neolacto-series GSLs. There is a report that human B cells contain nLc_4Cer (paragloboside) (23). In the present study, we demonstrated that three major GSL bands, which were detected by the 1B2-1B7 mAb after sialidase treatment, were absent from the splenocytes of *B3gnt5*$^{-/-}$ mice. This was confirmed by MS showing the absence of branching structures elongated on Lc_3Cer.

We investigated whether lacto/neolacto-series GSLs have an important role in biological functions, particularly in the immune system. The results indicated that *B3gnt5*$^{-/-}$ mice showed an enhanced response to BCR/CD19 stimuli. Recent studies have shown the importance of appropriate GEM formation for cell activation. Incorporation of a number of receptors, including the BCR, TCR, and GM1, into GEMs constitutes an important step in receptor function. After stimulation with various different agents, receptors and signaling molecules are incorporated into GEMs, effectively accumulate, and interact to result in signal transduction from the site of aggregation (i.e., GEMs). In T cells, aggregation of GEMs by cross-linking with CT-B, analogous to TCR cross-linking, induces signaling events and the respective signaling molecules are phosphorylated (24). We observed higher levels of CT-B staining (Fig. 2) and higher levels of GEM aggregation (Fig. 3) in resting *B3gnt5*$^{-/-}$ B cells, which could be the reason for their enhanced response to BCR stimulation. Because there were no differences in the total amount of GM1 and BCR-related molecules (e.g., BCR, CD19, Lyn), we hypothesize that some abnormalities or alterations of GEM microstructure might have occurred. We found that there was no increased expression of genes relating to the biosynthesis of GM1. This finding indicates that GM1 synthesis was not up-regulated at the level of gene expression. In addition, on the basis of the results of MS glycan analysis, as shown in Fig. 1 and Fig. S2, lacto/neolacto-series GSLs are present as a minor component of total GSLs. On the other hand, GM1 is the major component of total GSLs in mouse B cells. In fact, the pattern of MS spectra indicated no marked change in the amount of GM1, except for the decreased peak intensity related to lacto/neolacto-series GSLs. Nonetheless, the data raise the possibility that acceptor substrate (i.e., lactosylceramide) is shifted from the lacto/neolacto-series GSL synthetic pathway to the GM1 synthetic pathway. However, lacto/neolacto-series GSLs are normally only minor components in total GSLs, and it is difficult to accept that they are the reason for the increase in GM1. MS analysis or orcinol staining on TLC is, in general, poorly quantitative. Therefore, we performed TLC-immunoblotting as a more quantitative mode of analysis of GM1 GSL (Fig. S6). The results demonstrated that the total amount of GM1 did not differ between WT and *B3gnt5*$^{-/-}$ mice.

Concerning the brighter CT-B staining, we speculate that the alteration of GEM microstructure may cause the "unmasking" of GM1. Another possibility is that the alteration of GEM microstructure may affect the accessibility of GM1 molecules for CT-B. The clustering effect of GM1, caused by the ease of patching of GEM, may enhance the staining of CT-B. By immunoblotting, we observed slightly increased CT-B staining in separated GEM fractions. We interpret this as the result of the biochemical isolation of GM1 in clustered (patched) GEMs, as shown in Fig. 3. It is known that the microstructure of GEMs reflects their biochemical characteristics and that GM1 in clustered GEMs differs from monomolecular GM1. In general, lectin-like proteins, which can bind to glycans, exhibit stronger affinity to multivalent ligands than to monovalent ligands. CT-B is also known to form pentamer structures (25). It is possible that the clustered GEMs might be easily (and strongly) stained with CT-B in Figs. 2 and 3. However, we have not obtained enough evidence to explain the changes in GEM microstructure at this time. Although GEMs have been studied by a large number of groups, relatively little is known about their biochemical characteristics. Further study is therefore required to identify the detailed biological functions of ganglioside and GEMs.

One important issue in GEM function is their aggregation. There is now a consensus that GEMs are too small to be observed by light microscopy before stimulation (26). It is also reported that GEM formation is reversible, so that they exist only as transiently stabilized structures. GEMs can coalesce on clustering of their components, such as the BCR in B cells, with ligands, antibodies, and/or proteins having lectin activity. The small individual GEMs cluster into larger, visible, and functional units; such clustering facilitates efficient interaction of GEM-associated proteins. In the case of GPI-anchored proteins, such as CD59, dynamic and transient recruitment of GM1 to CD59 clusters was observed by single-molecule tracking and taken to suggest the involvement of GEMs in signal transduction (27). In this case, to form GEMs, clustering of such receptor molecules causes gathering of cholesterol and GSLs, such as GM1, around themselves. On the other hand, cross-linking of GM1 induces patching on the cell surface, resulting in signal transduction. Disruption of GEMs inhibits cell activation (13). Thus, both the association of receptor complexes and the platform of clustered GEMs are important for signaling via the GEMs. *B3gnt5*$^{-/-}$ resting B cells showed enlarged GM1 patches on their surface, resulting in increased BCR clustering. We observed no significant differences regarding the ratio of leukocyte populations in blood between WT and *B3gnt5*$^{-/-}$ mice. However, the data at 0 min in Fig. 5 showed that phosphorylation signals were slightly up-regulated in intact *B3gnt5*$^{-/-}$ B cells, and we found that Igs in serum were slightly increased in *B3gnt5*$^{-/-}$ mice (Fig. S4). We interpret these data as implying that the clustering of GEMs containing GM1 occurred more readily in *B3gnt5*$^{-/-}$ B cells than in WT B cells. The in vivo response of B cells to TI-II antigen (TNP) was more rapid and was slightly up-regulated in *B3gnt5*$^{-/-}$ B cells as compared with WT B cells (Fig. 5*C*). This result indicated that *B3gnt5*$^{-/-}$ B cells could be activated more easily than WT B cells.

We speculated that the up-regulation of GM1 clustering caused by the absence of PLN chains from GSLs depends on structural alterations at the cell surface, such as changes in lattice structures. These structures, consisting of galectin-carbohydrate cross-linked on the cell surface, regulate signal transduction through receptor segregation and turnover, and they also modulate cellular interaction (28). Their formation on the cell surface depends on galectin binding to LacNAc (Gal) residues on glycoproteins and GSLs (28, 29). However, the formation of lattice structures is proposed to occur only via glycoprotein–glycoprotein interactions. On the other hand, Galectin-1 can bind to GM1 and 1B2–1B7-reactive GSL-containing PLN chains (30). These interactions mainly result in inhibitory effects on the diffusion of receptor molecules and small GEMs. The decreased lattice structures in *B3gnt5*$^{-/-}$ B cells may be attributable to lectin-mediated interactions of GSLs-GSLs, and/or glycoproteins-GSLs, and may cause the rapid aggregation of GEMs. In *B3gnt5*$^{-/-}$ resting B cells, the small GEMs can easily aggregate into larger units when receptor complexes are formed. Thus, B3gnt5$^{-/-}$ B cells also exhibit up-regulated phosphorylation signals and hyperproliferation, as shown in this study. Galetin-1 negatively regulates B cell proliferation and Tyr-phosphorylation on BCR stimulation (31). Marked up-regulation of galectin-1 (*Lgals1*) and galectin-3 (*Lgals3*) gene expression has been demonstrated in anergic B cells (32). These data suggest that interactions of galectins and glycans may also play a role in the regulation of immune tolerance. Dissecting the detailed mechanisms responsible for enhanced GEM formation in *B3gnt5*$^{-/-}$ B cells is an attractive subject for future study.

In addition, we observed that the behavior of BCR and BCR-related molecules was different between WT and *B3gnt5*$^{-/-}$ B cells in the GEM fraction. As seen in Fig. 4 and Fig. S7, BCR and the signaling molecule Lyn are more abundant in the GEMs of *B3gnt5*$^{-/-}$ B cells than in those of WT B cells, and thus seem to be up-regulated on translocation of these molecules into GEMs. In Fig. 4, fractions 1–4 are observed as CT-B–positive bands in both WT and *B3gnt5*$^{-/-}$ B cells. We observed that the expression pattern of BCR, CD19, and Lyn corresponds to the GEM frac-

tion, which suggests the incorporation of these molecules into GEMs. We thought that these molecules move into the GEM fractions. There is a large amount of these molecules in GEMs of *B3gnt5*$^{-/-}$ B cells stimulated with anti-CD19 Ab alone (Fig. S7). This observation also indicates that GEM-related molecules, such as BCR, CD19, and Lyn, seem to be translocated into GEMs. Alternatively, it is clear that a large amount of BCR molecules exists in the GEM fraction in *B3gnt5*$^{-/-}$ B cells as compared with WT B cells. This result reflects the state of increased ease of activation in *B3gnt5*$^{-/-}$ B cells as compared with WT B cells.

We also think that there is no possibility that expression of BCR, CD19, or Lyn was up-regulated in B cell lysates. As shown in Fig. 2, there is no difference in the cell surface expression of these molecules between WT and *B3gnt5*$^{-/-}$ B cells, as quantified by FCM analysis. In addition, Western blotting data on their presence in B cell lysates (Fig. S5) showed that the amount of these molecules did not differ between WT and *B3gnt5*$^{-/-}$ mice. However, Fig. 4 shows that the amount of BCR and/or CD19 protein in non-GEM fractions might be slightly increased. Before isolation of the GEM fraction, the lysates were separated by brief centrifugation at maximum speed to exclude nuclei and some cytoskeleton proteins, including actin. It has been reported that BCR molecules associate with certain cytoskeletal proteins; for example, cytoskeleton components, such as actin, associate with GEMs or GEM proteins, such as BCR. Actin polymerization regulates the strength of BCR stimulation (33, 34). Therefore, during this procedure, it is possible that the interaction between BCR molecules and the cytoskeleton might be affected by any alteration of GEM structure. However, we have no data to explain this difference directly at this time. In this case, it is difficult to be sure that total BCR staining is equivalent in WT and *B3gnt5*$^{-/-}$ B cells. In this study, we focused attention on the difference in the behavior of these molecules around the center or adjacent fractions of GEMs between WT and *B3gnt5*$^{-/-}$ mice.

There are at least two possible molecular mechanisms that could be responsible for the phenomenon observed in *B3gnt5*$^{-/-}$ B cells. First, BCR–CD19 complexes are transferred efficiently into GEMs, because many more clustered GEMs are formed in *B3gnt5*$^{-/-}$ B cells than in WT B cells. Second, PLN on GSLs may control the behavior of glycoprotein entry into or exclusion from GEMs. To test this hypotheses, we would need to elucidate further which molecular interactions are altered by GSL-(poly)lactosamine deficiency. The results presented here suggest that PLN on GSLs is a putative immune regulatory factor. PLN chains on GSLs may have an important role in suppression of excessive responses in the immune system in the same manner as PLN on *N*-glycans of glycoprotein. The deletion of a specific glycosyltransferase gene in knockout mice indicates that some glycosyltransferases are essential for immune system integrity. In the present study, we revealed that lacto/neolacto-series GSLs might also have significant effects on biological function in the immune system.

Experimental Procedures

Detailed information on the experimental procedures of this study, including generating *B3gnt5*-deficient mice, extraction of GSLs, glycan analysis, FCM analysis, fluorescence microscopy analysis, fractionation of GEMs, immunoblotting, cell proliferation assays, T-independent Ab production, and others, is provided in *SI Experimental Procedures and Results*. Materials, including the Abs and probes used, and glycosphingolipid structures are also described in *SI Experimental Procedures and Results*.

ACKNOWLEDGMENTS. We thank Dr. Hiroyasu Ishida of Tsukuba University and Ms. Mihou Fushimi of the National Institute of Advanced Industrial Science and Technology for excellent assistance. This work was supported by the New Energy and Industrial Technology Development Organization (NEDO).

1. Prinetti A, Loberto N, Chigorno V, Sonnino S (2009) Glycosphingolipid behaviour in complex membranes. *Biochim Biophys Acta* 1788:184–193.
2. Yohe HC, Coleman DL, Ryan JL (1985) Ganglioside alterations in stimulated murine macrophages. *Biochim Biophys Acta* 818:81–86.
3. Simons K, Ikonen E (1997) Functional rafts in cell membranes. *Nature* 387:569–572.
4. Brown DA, London E (2000) Structure and function of sphingolipid- and cholesterol-rich membrane rafts. *J Biol Chem* 275:17221–17224.
5. Hakomori S (2004) Glycosynapses: Microdomains controlling carbohydrate-dependent cell adhesion and signaling. *An Acad Bras Cienc* 76:553–572.
6. Smith DC, Lord JM, Roberts LM, Johannes L (2004) Glycosphingolipids as toxin receptors. *Semin Cell Dev Biol* 15:397–408.
7. Hakomori S (2004) Carbohydrate-to-carbohydrate interaction, through glycosynapse, as a basis of cell recognition and membrane organization. *Glycoconj J* 21:125–137.
8. Nishio M, Tajima O, Furukawa K, Urano T, Furukawa K (2005) Over-expression of GM1 enhances cell proliferation with epidermal growth factor without affecting the receptor localization in the microdomain in PC12 cells. *Int J Oncol* 26:191–199.
9. Anderson RG, Jacobson K (2002) A role for lipid shells in targeting proteins to caveolae, rafts, and other lipid domains. *Science* 296:1821–1825.
10. Petrie RJ, Schnetkamp PP, Patel KD, Awasthi-Kalia M, Deans JP (2000) Transient translocation of the B cell receptor and Src homology 2 domain-containing inositol phosphatase to lipid rafts: evidence toward a role in calcium regulation. *J Immunol* 165:1220–1227.
11. Razzaq TM, et al. (2004) Regulation of T-cell receptor signalling by membrane microdomains. *Immunology* 113:413–426.
12. Viola A, Schroeder S, Sakakibara Y, Lanzavecchia A (1999) T lymphocyte costimulation mediated by reorganization of membrane microdomains. *Science* 283:680–682.
13. Xavier R, Brennan T, Li Q, McCormack C, Seed B (1998) Membrane compartmentation is required for efficient T cell activation. *Immunity* 8:723–732.
14. Yuyama K, Sekino-Suzuki N, Sanai Y, Kasahara K (2003) Lipid rafts in cellular signaling and disease. *Trends Glycosci Glycotechnol* 15:139–151.
15. Miceli MC, et al. (2001) Co-stimulation and counter-stimulation: Lipid raft clustering controls TCR signaling and functional outcomes. *Semin Immunol* 13:115–128.
16. Togayachi A, Sato T, Narimatsu H (2006) Comprehensive enzymatic characterization of glycosyltransferases with a β3GT or β4GT motif. *Methods Enzymol* 416:91–102.
17. Togayachi A, et al. (2001) Molecular cloning and characterization of UDP-GlcNAc: lactosylceramide β1,3-*N*-acetylglucosaminyltransferase (β3Gn-T5), an essential enzyme for the expression of HNK-1 and Lewis X epitopes on glycolipids. *J Biol Chem* 276: 22032–22040.
18. Henion TR, Zhou D, Wolfer DP, Jungalwala FB, Hennet T (2001) Cloning of a mouse beta 1,3 *N*-acetylglucosaminyltransferase GlcNAc(beta 1,3)Gal(beta 1,4)Glc-ceramide synthase gene encoding the key regulator of lacto-series glycolipid biosynthesis. *J Biol Chem* 276:30261–30269.
19. Togayachi A, et al. (2007) Polylactosamine on glycoproteins influences basal levels of lymphocyte and macrophage activation. *Proc Natl Acad Sci USA* 104:15829–15834.
20. Biellmann F, Hülsmeier AJ, Zhou D, Cinelli P, Hennet T (2008) The Lc3-synthase gene B3gnt5 is essential to pre-implantation development of the murine embryo. *BMC Dev Biol* 8:109.
21. Tsubata T (1999) Co-receptors on B lymphocytes. *Curr Opin Immunol* 11:249–255.
22. Kovacic N, Müthing J, Marusic A (2000) Immunohistological and flow cytometric analysis of glycosphingolipid expression in mouse lymphoid tissues. *J Histochem Cytochem* 48: 1677–1690.
23. Schwarting GA (1980) Quantitative analysis of neutral glycosphingolipids from human lymphocyte subpopulations. *Biochem J* 189:407–412.
24. Janes PW, Ley SC, Magee AI (1999) Aggregation of lipid rafts accompanies signaling via the T cell antigen receptor. *J Cell Biol* 147:447–461.
25. Ruddock LW, et al. (1996) A pH-dependent conformational change in the B-subunit pentamer of Escherichia coli heat-labile enterotoxin: Structural basis and possible functional role for a conserved feature of the AB5 toxin family. *Biochemistry* 35: 16069–16076.
26. Pralle A, Keller P, Florin EL, Simons K, Hörber JK (2000) Sphingolipid-cholesterol rafts diffuse as small entities in the plasma membrane of mammalian cells. *J Cell Biol* 148: 997–1008.
27. Suzuki KG, Fujiwara TK, Edidin M, Kusumi A (2007) Dynamic recruitment of phospholipase C gamma at transiently immobilized GPI-anchored receptor clusters induces IP3-Ca2+ signaling: single-molecule tracking study 2. *J Cell Biol* 177:731–742.
28. Rabinovich GA, Toscano MA, Jackson SS, Vasta GR (2007) Functions of cell surface galectin-glycoprotein lattices. *Curr Opin Struct Biol* 17:513–520.
29. Garner OB, Baum LG (2008) Galectin-glycan lattices regulate cell-surface glycoprotein organization and signalling. *Biochem Soc Trans* 36:1472–1477.
30. Elola MT, Chiesa ME, Alberti AF, Mordoh J, Fink NE (2005) Galectin-1 receptors in different cell types. *J Biomed Sci* 12:13–29.
31. Yu X, Siegel R, Roeder RG (2006) Interaction of the B cell-specific transcriptional coactivator OCA-B and galectin-1 and a possible role in regulating BCR-mediated B cell proliferation. *J Biol Chem* 281:15505–15516.
32. Clark AG, et al. (2007) Multifunctional regulators of cell growth are differentially expressed in anergic murine B cells. *Mol Immunol* 44:1274–1285.
33. Brown BK, Song W (2001) The actin cytoskeleton is required for the trafficking of the B cell antigen receptor to the late endosomes. *Traffic* 2:414–427.
34. Hao S, August A (2005) Actin depolymerization transduces the strength of B cell receptor stimulation. *Mol Biol Cell* 16:2275–2284.

INFECTION AND IMMUNITY, May 2010, p. 2302–2311 Vol. 78, No. 5
0019-9567/10/$12.00 doi:10.1128/IAI.01398-09

Impairment of Host Defense against Disseminated Candidiasis in Mice Overexpressing GATA-3[▽]

Norihiro Haraguchi,[1] Yukio Ishii,[1]* Yuko Morishima,[1] Keigyou Yoh,[2] Yosuke Matsuno,[1] Norihiro Kikuchi,[1] Tohru Sakamoto,[1] Satoru Takahashi,[3] and Nobuyuki Hizawa[1]

Department of Respiratory Medicine[1] and Department of Nephrology, Institute of Clinical Medicine,[2] and Laboratory Animal Resource Center,[3] University of Tsukuba, 1-1-1 Tennoudai, Tsukuba, Ibaraki 305-8575, Japan

Received 16 December 2009/Returned for modification 6 January 2010/Accepted 5 March 2010

***Candida* species are the most common source of nosocomial invasive fungal infections. Previous studies have indicated that T-helper immune response is the critical host factor for susceptibility to *Candida* infection. The transcription factor GATA-3 is known as the master regulator for T-helper type 2 (Th2) differentiation. We therefore investigated the role of GATA-3 in the host defense against systemic *Candida* infection using GATA-3-overexpressing transgenic mice. The survival of GATA-3-overexpressing mice after *Candida* infection was significantly lower than that of wild-type mice. *Candida* outgrowth was significantly increased in the kidneys of GATA-3-overexpressing mice, compared with wild-type mice. The levels of various Th2 cytokines, including interleukin-4 (IL-4), IL-5, and IL-13, were significantly higher while the level of Th1 cytokine gamma interferon was significantly lower in the splenocytes of GATA-3-overexpressing mice after *Candida* infection. Recruitment of macrophages into the peritoneal cavity in response to *Candida* infection and their phagocytic activity were significantly lower in GATA-3-overexpressing mice than in wild-type mice. Exogenous administration of gamma interferon to GATA-3-overexpressing mice significantly reduced *Candida* outgrowth in the kidney and thus increased the survival rate. Administration of gamma interferon also increased the recruitment of macrophages into the peritoneal cavity in response to *Candida* infection. These results indicate that overexpression of GATA-3 modulates macrophage antifungal activity and thus enhances the susceptibility to systemic *Candida* infection, possibly by reducing the production of gamma interferon in response to *Candida* infection.**

Candida albicans is an opportunistic fungal pathogen causative of the most widespread nosocomial bloodstream infections worldwide (25, 35). *Candida* is part of the normal microbial flora in human beings and domestic animals and is associated with mucosal surfaces of the oral cavity, gastrointestinal tract, and vagina. However, under conditions of immune dysfunction, *Candida* switches from a commensal to a pathogenic organism capable of infecting a variety of tissues and can subsequently cause fatal systemic diseases (2, 7).

Several host factors involved in the innate and adaptive immune systems are required for the systemic control of *Candida* infection. In mice, resistance and susceptibility to systemic *Candida* infection may be linked, at least in part, to the dissimilar expansion of functionally distinct CD4-positive T-cell subsets. Previous studies have demonstrated that resistance to *Candida* infection is associated with T-helper type 1 (Th1) immunity, whereas type 2 (Th2) immunity is associated with susceptibility to symptomatic infection (28, 29). Activation of innate immunity, such as the ability of phagocytic cells to inhibit fungal growth, is required for the induction of Th1 cells (19, 20). The Th1 cytokine gamma interferon (IFN-γ) is required for optimal activation of phagocytes such as neutrophils and macrophages, collaborates in the generation of protective antibody response, and favors the development of a Th1 protective response (9). Early in *Candida* infection, another Th1 cytokine, tumor necrosis factor alpha (TNF-α), is also essential for the successful control of the infection and the resulting protective Th1-dependent immunity (28). In contrast, Th2 cytokines, such as interleukin-4 (IL-4) and IL-10, inhibit Th1 development and deactivate phagocytic effector cells.

Th1 and Th2 cells are differentiated from common T precursor cells (1, 16), and their differentiation requires the activity of distinct transcription factors. Among a variety of key molecules governing Th1/Th2 differentiation, GATA-3 has been implicated in Th2 commitment (22, 34, 37, 39). Under physiological conditions, GATA-3 is selectively expressed in Th2 but not Th1 cells (37, 38, 39). Transgenic and retroviral expression of GATA-3 induces a Th2 cytokine profile in Th1 cells (37, 39), while dominant-negative GATA-3 downregulates Th2 clones (38). GATA-3 is now recognized as a master regulator for Th2 cell differentiation. It is therefore likely that GATA-3 is a critical host factor in the determination of susceptibility to systemic *Candida* infection.

We recently established GATA-3-overexpressing transgenic (*GATA-3-tg*) mice. In the present study, we investigate the role of GATA-3 in the host defense against disseminated candidiasis using these mice.

MATERIALS AND METHODS

Mice. *GATA-3-tg* mice were generated as previously described (36). *GATA-3-tg* mice were backcrossed with C57BL/6 mice for eight generations, and the sufficiency of backcross was confirmed by analyzing the polymorphism of microsatellite DNAs. The genetic background was uniformized to C57BL/6 by backcrossing for eight generations. C57BL/6 wild-type (WT) mice were purchased

* Corresponding author. Mailing address: Department of Respiratory Medicine, University of Tsukuba, 1-1-1 Tennoudai, Tsukuba, Ibaraki 305-8575, Japan. Phone and fax: 81-298-53-3144. E-mail: ishii-y@md.tsukuba.ac.jp.

▽ Published ahead of print on 15 March 2010.

from Charles River Breeding Laboratories (Kanagawa, Japan). All mice used in this study were 8 to 12 weeks old and were maintained in our animal facilities under specific-pathogen-free conditions. All animal studies were approved by the Institutional Review Board.

***Candida* infection model.** *C. albicans* was obtained from the American Type Culture Collection (Manassas, VA). Mice were infected by intraperitoneal inoculation of 1×10^5 *Candida* blastoconidia in 500 μl of sterile pyrogen-free phosphate-buffered saline (PBS) isolated from fungal cultures made in YM broth (Difco Laboratories, Detroit, MI) for 48 h at 24°C. The survival of mice after *C. albicans* infection was assessed daily for 56 days. At 1, 3, 7, 30, and 56 days after the inoculation, the blood and organs (i.e., lung, heart, liver, spleen, and kidney) were removed aseptically. Quantification of *C. albicans* was performed by plating several dilutions of homogenized organs in Sabouraud dextrose agar. The results were expressed as $\log_{10}$ CFU per organ. For the histological analysis, the tissues were immediately fixed in formalin. Sections (4 μm) of paraffin-embedded tissues were stained with periodic acid-Schiff (PAS) reagent.

Peritoneal cell lavage. The peritoneal cavity was lavaged with five sequential 2-ml aliquots of PBS. The cells were centrifuged and resuspended in PBS. Cells were counted using a hemocytometer, and a differential cell count was performed by standard light microscopic techniques. The percentage of macrophages and neutrophils phagocytosing *C. albicans* was evaluated by staining with PAS reagent. A minimum of 300 cells were evaluated in each preparation. To obtain peritoneal macrophages, the cells were stained with anti-F4/80 antibody (BD PharMingen, San Diego, CA) and were sorted with a MoFlo flow cytometry system using Summit software (Beckman Coulter, Inc., Brea, CA).

RT-PCR. The expression levels of IFN-γ, TNF-α, IL-4, IL-5, IL-13, monocyte chemotactic protein 1 (MCP-1), keratinocyte-derived chemokine (KC), and macrophage inflammatory protein 2 (MIP-2) genes were determined by quantitative real-time reverse transcription-PCR (RT-PCR) using ready-made fluorogenic probes and primers (Applied Biosystems, Foster City, CA). Expression levels for amplicons were quantified using the threshold cycle ($\Delta\Delta C_T$) method according to the manufacturer's protocols. The expression levels were normalized against 18S rRNA.

Flow cytometry. Seven days after *C. albicans* inoculation, the spleen was removed, minced, and passed through a fine steel mesh to obtain a homogeneous cell suspension. Erythrocytes were hemolyzed by using NH_4Cl solution. The residual cells were then filtered through a 20-μm nylon mesh. Cells were stained with anti-T-cell receptor β (anti-TCRβ), anti-CD4, and anti-CD8 (BD PharMingen) and anti-CXCR3 and anti-CCR3 (R&D Systems, Inc., Minneapolis, MN). After being stained, the cells were analyzed by flow cytometry using a FACSCalibur with CellQuest software (Biosciences, San Jose, CA).

Intracellular cytokine analysis. Levels of IFN-γ production in splenocytes were determined by flow cytometric intracellular cytokine analysis as previously described (21). Briefly, the cells were resuspended in RPMI 1640 containing 10% fetal calf serum (FCS), incubated with phorbol myristate acetate (PMA; 50 ng/ml; Sigma-Aldrich) and ionomycin (500 ng/ml; Sigma) for 2 h, and then incubated with brefeldin A (10 μg/ml; Sigma) for 2 h at 37°C. The cells were stained with phycoerythrin (PE)-conjugated anti-mouse IFN-γ antibody (BD PharMingen) and fixed with 2% paraformaldehyde–PBS solution. Data were analyzed by flow cytometry.

Supplementation with IFN-γ. *GATA-3-tg* mice were daily treated with 8×10^6 U of murine recombinant IFN-γ (BD PharMingen) or diluent subcutaneously for 14 consecutive days.

Statistics. Data were expressed as the means ± standard errors of the means (SEM). Comparisons of data among the experimental groups were performed using the analysis of variance and Scheffe's test. The survival curves were analyzed using the log-rank test. Values of $P < 0.05$ were considered to be statistically significant.

RESULTS

Overexpression of GATA-3 enhances susceptibility to *C. albicans*. We first assessed the survival rate following infection of WT mice and *GATA-3-tg* mice with *C. albicans*. The mortality of *GATA-3-tg* mice was significantly higher than that of WT mice after either intraperitoneal inoculation or intravenous inoculation of *C. albicans*. Sixty percent of *GATA-3-tg* mice died while 25% of the WT mice died within 56 days after the intraperitoneal inoculation (Fig. 1A). Intravenous fungal inoculation caused early death in both genotypes of mice, compared with intraperitoneal inoculation. All *GATA-3-tg* mice died within 15 days while 50% of the WT mice survived to 18 days after the intravenous inoculation (Fig. 1B). No mice died in the saline-administered control group of either genotype (Fig. 1A and B).

Overexpression of GATA-3 enhances systemic candidiasis. We next assessed the growth and systemic spread of *C. albicans* in WT mice and *GATA-3-tg* mice. The outgrowth of *C. albicans* was most frequent in the kidney of *GATA-3-tg* mice after infection by either the intraperitoneal or intravenous route. *Candida* CFU per tissue were significantly higher in the kidneys of *GATA-3-tg* mice than in those of WT mice at 56 days post-intraperitoneal inoculation (Fig. 2A). *Candida* outgrowth was detected in all kidneys and 5/10 lungs of *GATA-3-tg* mice, whereas it was detected in none of the kidneys and 1/10 lungs of WT mice at that time point (Table 1). *C. albicans* was detected in all lungs and kidneys of both genotypes of mice at 14 days post-intravenous inoculation (Table 1). However, *Candida* CFU per tissue were significantly higher in both the lungs and kidneys of *GATA-3-tg* mice than in those of WT mice at that time point (Fig. 2B).

Histopathological analysis also revealed severe renal damage with bilateral hydronephrosis in *GATA-3-tg* mice after *C. albicans* infection via either an intraperitoneal or an intravenous route (Fig. 2C, GATA3-tg). Marked fungal growth with hyphal formation was observed with the infiltration of numerous inflammatory cells into the pelvis of *GATA-3-tg* mice (Fig. 2C, inset). In contrast, the damage was much less severe and no obvious hydronephrosis was observed in the kidneys of WT mice infected via either an intraperitoneal or an intravenous route (Fig. 2C, WT).

Cytokine expression is deviated toward Th2 in GATA-3-overexpressing mice after *C. albicans* infection. To clarify the contribution of GATA-3 overexpression to Th1/Th2 balance after *C. albicans* infection, we evaluated the expression of both Th1 and Th2 cytokines in the splenocytes of WT mice and *GATA-3-tg* mice after fungal inoculation. The expression of the Th1 cytokine IFN-γ was elevated in the splenocytes of WT mice after the inoculation. The level of IFN-γ was significantly higher in the splenocytes of WT mice than in those of *GATA-3-tg* mice at 3, 7, and 30 days postinoculation (Fig. 3; IFN-γ). The expression of TNF-α was elevated in the splenocytes of *GATA-3-tg* mice 3 days postinoculation, and the level of TNF-α was significantly higher in WT mice than in *GATA-3-tg* mice at that time point (Fig. 3, TNF-α). On the other hand, the expression of Th2 cytokine IL-4 was elevated in the splenocytes of *GATA-3-tg* mice but not those of WT mice after *C. albicans* inoculation. The IL-4 level in *GATA-3-tg* mice was significantly higher than that in WT mice at 3, 7, and 30 days postinoculation (Fig. 3, IL-4). The levels of IL-5 and IL-13 were also significantly higher in the splenocytes of *GATA-3-tg* mice than in those of WT mice at 7 and 30 days postinoculation (Fig. 3, IL-5 and IL-13). These results indicate that *GATA-3-tg* mice are highly biased toward Th2 due to impaired induction of IFN-γ and enhanced induction of IL-4, IL-5, and IL-13 after *Candida* infection.

The production of IFN-γ is reduced in Th1 cells in GATA-3-overexpressing mice after *C. albicans* infection. Previous studies demonstrated that IFN-γ plays an important role in protection against *Candida* infection. We assessed the IFN-γ

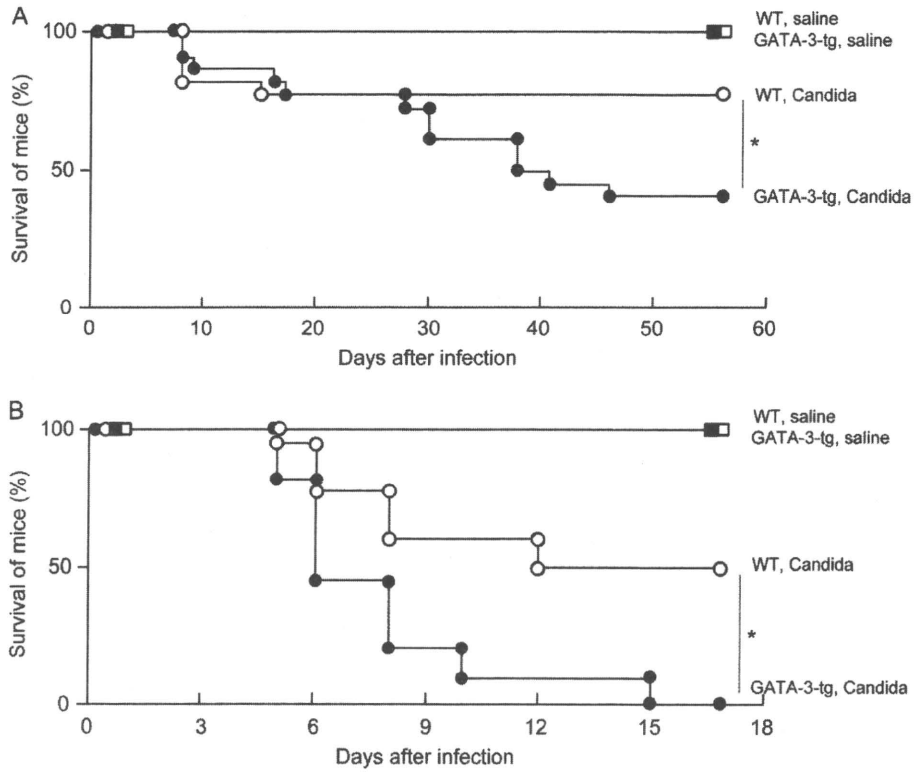

FIG. 1. (A) Survival of wild-type (WT; open symbols) mice and GATA-3-overexpressing (GATA-3-tg; closed symbols) mice after intraperitoneal inoculation of 1×10^8 CFU of *Candida albicans* (circles) or saline (squares). (B) Survival of WT (open symbols) mice and GATA-3-overexpressing (GATA-3-tg; closed symbols) mice after intravenous inoculation of 1×10^6 CFU of *Candida albicans* (circles) or saline (squares). *, significantly different between wild-type mice and GATA-3-overexpressing mice ($P < 0.05$; $n = 20$ in each group).

production ability of the splenocytes of WT mice and *GATA-3-tg* mice. We first evaluated the ratio of CD4- to CD8-positive T cells in the spleens of both WT mice and *GATA-3-tg* mice before and 7 days postinoculation. The ratio of CD4- to CD8-positive cells was not different between the genotypes irrespective of *Candida* infection (Fig. 4A). In both genotypes of mice, the number of CD4-positive cells was three to four times greater than that of CD8-positive cells. We then assessed the proportion of IFN-γ-producing cells among CD4- and CD8-positive cells. The proportion of IFN-γ-producing cells in CD4-positive cells increased after *Candida* inoculation in WT mice but not in *GATA-3-tg* mice. The proportion was significantly higher in WT mice than in *GATA-3-tg* mice before and 7 days postinoculation (Fig. 4B, left panel). The proportion of IFN-γ-producing cells in CD8-positive cells was not different between the genotypes irrespective of *Candida* infection (Fig. 4B, right panel). We then assessed the proportion of CXCR3-positive cells and CCR3-positive cells in CD4-positive cells; these are the cell surface markers of Th1 and Th2 cells, respectively. The proportion of CXCR3-positive cells was not different between the genotypes before *Candida* inoculation. The proportion of CXCR3-positive cells decreased significantly in *GATA-3-tg* mice but not in WT mice 7 days postinoculation (Fig. 4C, left panel). Therefore, the proportion of CXCR3-positive cells was significantly higher in WT mice than in *GATA-3-tg* mice at that time point (Fig. 4C, left panel). The proportion of CCR3-positive cells was not different between the genotypes either before or 7 days postinoculation (Fig. 4C, right panel). We further assessed the proportion of IFN-γ-producing cells in CXCR3-positive cells. The proportion increased after *Candida* infection in WT mice but not in *GATA-3-tg* mice. The proportion was significantly higher in WT mice than in *GATA-3-tg* mice 7 days postinoculation (Fig. 4D).

Response of macrophages to *C. albicans* is impaired in GATA-3-overexpressing mice. We then assessed inflammatory cell infiltration into the peritoneal cavity, the site of infection. The number of total lavageable cells was increased in WT mice but not in *GATA-3-tg* mice 7 days postinoculation, compared with the number before inoculation (Fig. 5A, total cells). The number of total lavageable cells was significantly higher in WT mice than in *GATA-3-tg* mice at that time point (Fig. 5A, total cells). The number of macrophages was also significantly higher in WT mice than in *GATA-3-tg* mice 7 days postinoculation (Fig. 5A, macrophages). No difference in the number of neutrophils or lymphocytes was observed between genotypes (Fig. 5A, neutrophils and lymphocytes). Since the number of macrophages was increased in response to *Candida* infection in the peritoneal cavity of WT mice, we next assessed the expression of chemokines in peritoneal macrophages. Although the expression of MCP-1, a CC chemokine, was elevated in peritoneal macrophages of both genotypes 7 days postinoculation, the expression level was significantly higher in peritoneal macro-

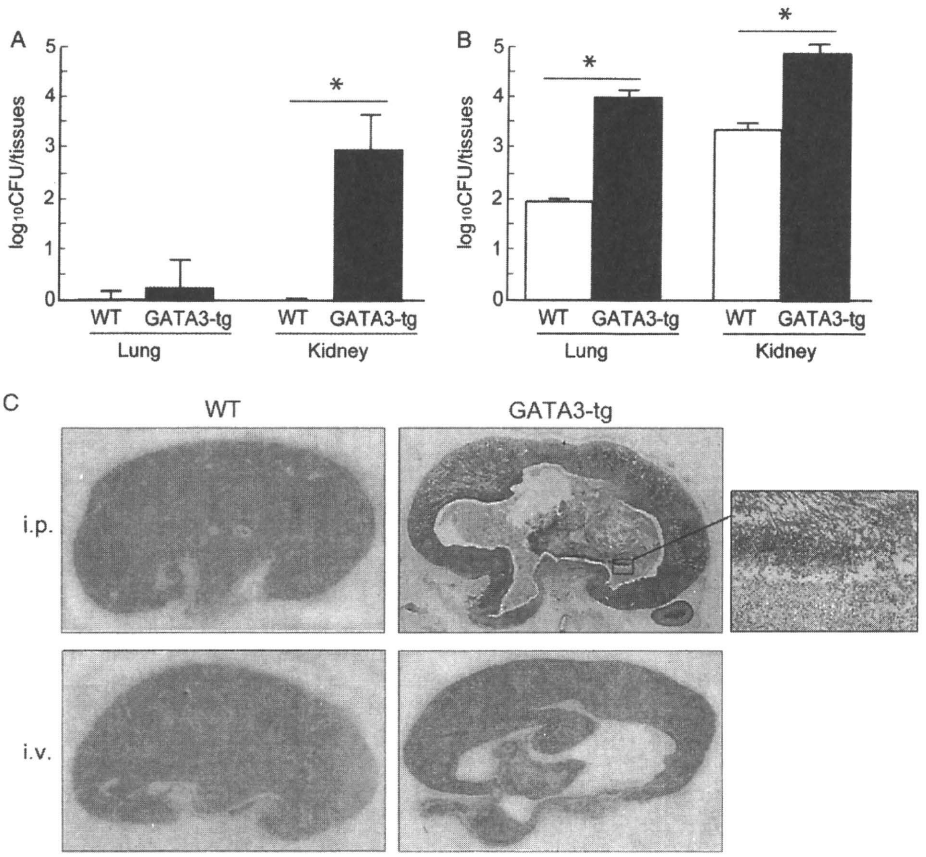

FIG. 2. Evaluation of systemic *Candida* infection in wild-type mice and GATA-3-overexpressing mice. Outgrowth of *Candida albicans* in the lungs and kidneys of wild-type (WT) mice and GATA-3-overexpressing mice (GATA3-tg) 56 days after intraperitoneal inoculation of *Candida albicans* (A) and 14 days after intravenous inoculation of *Candida albicans* (B) is shown. The results are expressed as $\log_{10}$ CFU per organ. The experiments were performed in duplicate with five mice in each group. *, significantly different between wild-type mice and GATA-3-overexpressing mice ($P < 0.05$). (C) Histopathology of the kidneys of WT mice and GATA-3-overexpressing (GATA3-tg) mice 56 days after intraperitoneal inoculation (i.p.) or 14 days after intravenous inoculation (i.v.) of *Candida albicans*. Severe hydronephrosis is seen in *GATA-3-tg* mice but not in WT mice. The boxed area, magnified in the inset, shows *Candida albicans* colonies with numerous inflammatory cells. PAS staining. Representative photographs of the kidneys from 8 mice in each group are shown (magnification, ×10 [inset, ×100]).

phages of WT mice than in those of *GATA-3-tg* mice (Fig. 5B, MCP-1). Similarly, the expression levels of KC and MIP-2, macrophage-derived CXC chemokines, were significantly higher in peritoneal macrophages of WT mice than in those of *GATA-3-tg* mice 7 days postinoculation (Fig. 5B, KC and MIP-2).

We further assessed phagocytic activity of peritoneal macrophages and neutrophils histologically. The engulfment of *C. albicans* by both macrophages and neutrophils was observed most frequently at 3 days postinoculation in both genotypes of mice (Fig. 6A). However, the numbers of macrophages and neutrophils phagocytosing *C. albicans* were significantly higher in *GATA-3-tg* mice than in WT mice both 3 days and 7 days postinoculation (Fig. 6B and C).

TABLE 1. Fungal growth in each organ post-inoculation of *C. albicans*[a]

Inoculation route	No. of positive mice/total no. of mice			
	Wild-type mice		*GATA-3-tg* mice	
	Lung	Kidney	Lung	Kidney
i.p.	1/10	0/10	5/10	10/10
i.v.	10/10	10/10	10/10	10/10

[a] The fungal growth was evaluated 56 days after intraperitoneal (i.p.) inoculation and 14 days after intravenous (i.v.) inoculation of *Candida albicans*.

Supplementation with IFN-γ improves the degree of systemic candidiasis in GATA-3-overexpressing mice. Because the production of IFN-γ was significantly lower in the spleen and its CD4- and CXCR3-positive cells in *GATA-3-tg* mice, we next assessed whether exogenous supplementation with IFN-γ would reduce the development of disseminated candidiasis. Mouse recombinant IFN-γ was administered to *GATA-3-tg* mice subcutaneously for 14 consecutive days. We first evaluated the survival rate following infection of *GATA-3-tg* mice with *C. albicans* with or without IFN-γ administration. The survival rate was significantly higher in *GATA-3-tg* mice treated with IFN-γ than in the vehicle-treated controls. Fifty-five percent of vehicle-treated *GATA-3-tg* mice died within 56 days postinoculation (Fig. 7A). However, the mortality was reduced to 30% in *GATA-3-tg* mice treated with IFN-γ (Fig. 7A). No

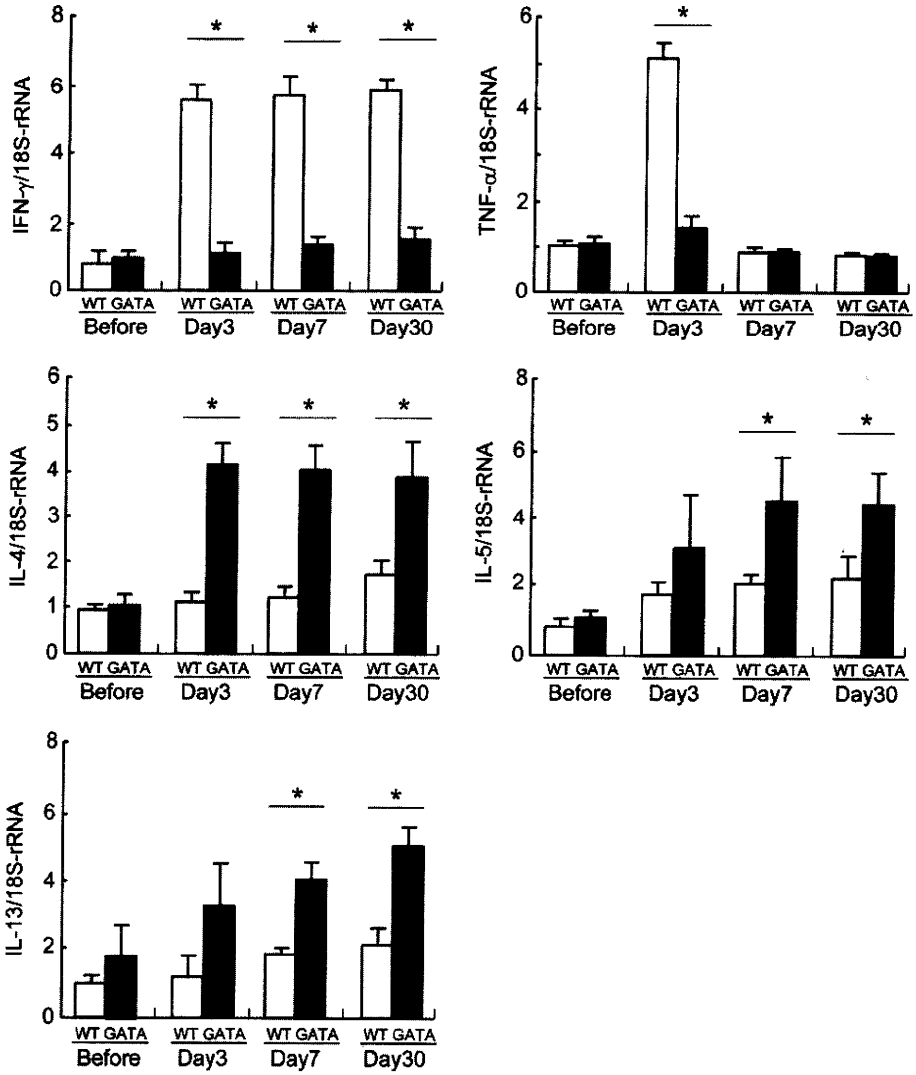

FIG. 3. The expression of IFN-γ, tumor necrosis factor-α (TNF-α), IL-4, IL-5, and IL-13 in the spleens of wild-type (WT) mice and GATA-3-overexpressing (GATA) mice before and at 3 (Day 3), 7 (Day 7), and 30 (Day 30) days after intraperitoneal inoculation of 1×10^8 CFU of *Candida albicans*. Experiments were performed in duplicate with five mice in each group. *, significantly different between wild-type mice and GATA-3-overexpressing mice ($P < 0.05$).

mice died in the saline-administered control group of either genotype (Fig. 7A). We next assessed the growth and systemic spread of *C. albicans* in *GATA-3-tg* mice with or without IFN-γ administration at 56 days postinoculation. The growth of *C. albicans* was most frequently observed in the kidney irrespective of IFN-γ administration (Fig. 7B). However, the degree of *Candida* outgrowth was much less severe in *GATA-3-tg* mice treated with IFN-γ than in those without IFN-γ administration (Fig. 7B). We further assessed inflammatory cell infiltration into the peritoneal cavity at 7 days after *Candida* inoculation with or without IFN-γ administration. The numbers of total lavageable cells and macrophages were significantly higher in *GATA-3-tg* mice treated with IFN-γ than in those not receiving IFN-γ administration (Fig. 7C, total cells and macrophages). No significant difference in the number of neutrophils and lymphocytes was observed between IFN-γ-treated and vehicle-treated mice (Fig. 7C, neutrophils and lymphocytes).

DISCUSSION

In the present study, we demonstrated for the first time that systemic infection with *C. albicans* is much more severe in *GATA-3-tg* mice than in WT mice of the same background. Analysis of cytokines revealed that overexpression of GATA-3 shifted the Th1/Th2 balance toward Th2 after *Candida* infection, whereas the balance was shifted to Th1 in WT mice by the same infection. GATA-3 is a member of the GATA family of zinc finger transcription factors, which bind the GATA consensus motif (11). As stated above, GATA-3 is best known to function as a master regulator of Th2 cell differentiation. In

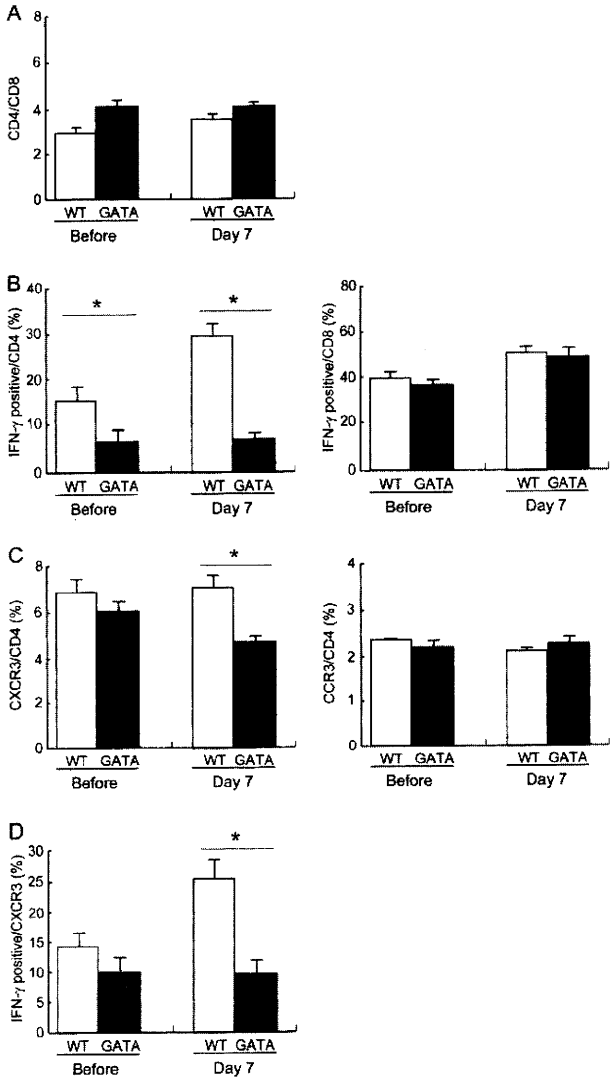

FIG. 4. (A) The ratio of CD4-positive cells to CD8-positive cells in the spleens of wild-type (WT) mice and GATA-3-overexpressing (GATA) mice before and 7 days (Day 7) after intraperitoneal inoculation of 1×10^8 CFU of *Candida albicans*. Experiments were performed in duplicate with five mice in each group. (B) The proportion of gamma-interferon-producing cells among CD4-positive cells (left panel) or among CD8-positive cells (right panel) in the spleens of wild-type (WT) mice and GATA-3-overexpressing (GATA) mice before and 7 days (Day 7) after intraperitoneal inoculation of 1×10^8 CFU of *Candida albicans*. Experiments were performed in duplicate with five mice in each group. (C) The proportion of CXCR3-positive cells (left panel) and CCR3-positive cells (right panel) among CD4-positive cells in the spleens of WT mice and GATA-3-overexpressing (GATA) mice before and 7 days (Day 7) after intraperitoneal inoculation of 1×10^8 CFU of *Candida albicans*. Experiments were performed in duplicate with five mice in each group. (D) The proportion of gamma-interferon-producing cells among CXCR3-positive cells in the spleens of WT mice and GATA-3-overexpressing (GATA) mice before and 7 days (Day 7) after intraperitoneal inoculation of 1×10^8 CFU of *Candida albicans*. Experiments were performed in duplicate with five mice in each group. *, significantly different between wild-type mice and GATA-3-overexpressing mice ($P < 0.05$).

addition to Th2 cell differentiation, GATA-3 plays a central role in Th2 cytokine production. It has been demonstrated that antisense GATA-3 inhibited the expression of all Th2 cytokine genes in the Th2 clone D10 (39). In transgenic mice, elevated GATA-3 in CD4-positive T cells caused Th2 cytokine gene expression in developing Th1 cells (39). GATA-3 has been reported to transactivate the IL-5 promoter with only limited effects on IL-4 gene transcription (24, 37, 38). It has also been reported that GATA-3 regulates the locus accessibility of the IL-4 and IL-13 genes with chromatin remodeling (15, 33). These findings suggest that GATA-3 allows the expression of Th2 cytokines by functioning as a transcription factor as well as by modifying the chromatin structure of these cytokines.

In the present study, the IFN-γ level was significantly lower in the spleen of *GATA-3-tg* mice than in that of WT mice after *Candida* infection. Several studies have demonstrated that GATA-3 not only transactivates Th2 cytokines but also suppresses Th1 cytokine expression. It was reported that GATA-3 significantly downregulated IFN-γ production during *in vitro* Th1 differentiation of naïve CD4-positive T cells through downregulation of IL-12 receptor β2 and IFN-γ production (8, 22). In contrast, IFN-γ production in $CD4^+$ T cells of GATA-3-deficient mice was increased even under a Th2 condition (23). GATA-3 suppresses IFN-γ gene transcription via the downregulation of signal transducer and activator of transcription 4 (STAT4) (12). In addition to suppression of IFN-γ gene transcription, GATA-3 inhibits IFN-γ production indirectly by inhibiting Th1 cell differentiation via repression of T-bet activation (10). Thus, it is reasonable to conclude that GATA-3 overexpression suppresses IFN-γ production in addition to upregulating Th2 cytokine production in the present model.

In the present study, exogenous administration of IFN-γ improved the degree of systemic *Candida* infection in *GATA-3-tg* mice. These findings suggest that the aggravation of *Candida* infection in *GATA-3-tg* mice is at least partly due to the reduction of IFN-γ production in response to *Candida* infection. Correspondingly, it has been reported that IFN-γ-knockout mice are highly susceptible to disseminated candidiasis induced by intraperitoneal inoculation of *C. albicans* blastoconidia with impairment of macrophage candidacidal activity (13). There is abundant evidence that IFN-γ is the major cytokine involved in activation of macrophages and neutrophils to a candidacidal stage (3, 9). The administration of IFN-γ to mice beneficially influences the course of experimental infection with various pathogens, such as *Toxoplasma gondii* (32), *Leishmania major* (17), *Trypanosoma cruzi* (6), and *Pneumocystis murina* (30). In most models, macrophages and/or neutrophils are the main effector cells of IFN-γ-stimulated microbicidal activity. Macrophages in particular play a key role in the innate immunity to *Candida* infections by engulfing, killing, and processing the pathogen for presentation to T cells. Consistent with these results, the phagocytic activity of macrophages and neutrophils was reduced in *GATA-3-tg* mice in the present study. In addition to phagocytosis, macrophages modulate immune and inflammatory responses by producing a number of cytokines, CC chemokines, and CXC chemokines.

MCP-1, also called CCL2, is a member of the CC chemokine family. MCP-1-mediated monocyte recruitment is essential for defense against various bacterial, protozoal, and fungal pathogens (31). KC and MIP-2, also called CXCL1 and CXCL2,

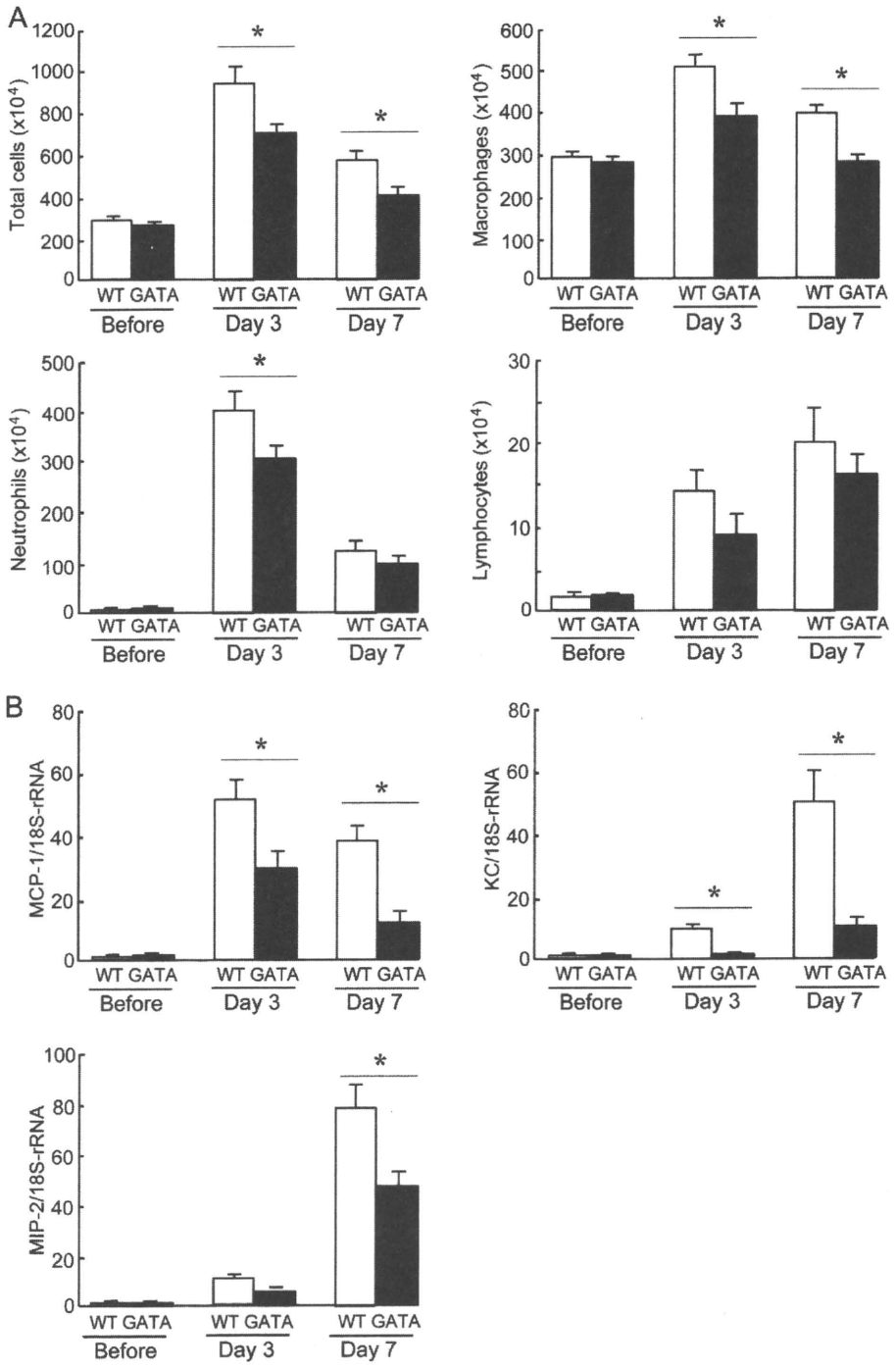

FIG. 5. (A) The number of total cells, macrophages, neutrophils, and lymphocytes in the peritoneal lavage fluids of wild-type (WT) mice and GATA-3-overexpressing (GATA) mice before and 3 days (Day 3) and 7 days (Day 7) after intraperitoneal inoculation of 1×10^8 CFU of *Candida albicans*. Experiments were performed in duplicate with five mice in each group. (B) The expression of monocyte chemotactic protein 1 (MCP-1), keratinocyte-derived chemokine (KC), and macrophage inflammatory protein 2 (MIP-2) in the peritoneal macrophages of WT mice and GATA-3-overexpressing (GATA) mice before and 3 days (Day 3) and 7 days (Day 7) after intraperitoneal inoculation of 1×10^8 CFU of *Candida albicans*. Experiments were performed in duplicate with five mice in each group. *, significantly different between wild-type mice and GATA-3-overexpressing mice ($P < 0.05$).

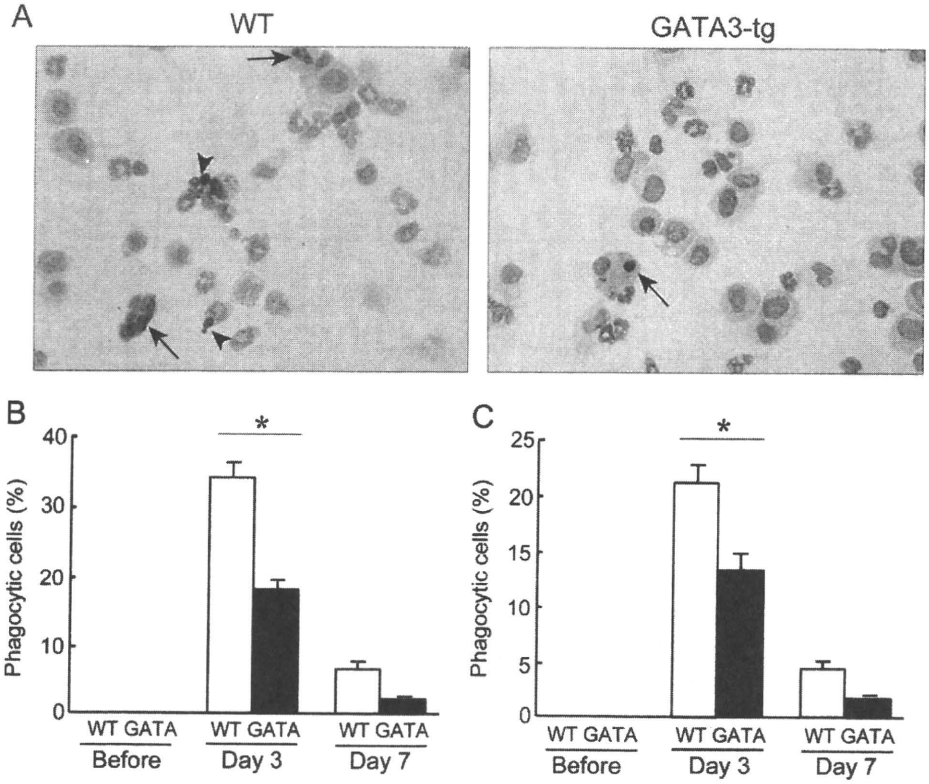

FIG. 6. (A) Representative photographs of peritoneal lavage cells 3 days after intraperitoneal inoculation of 1×10^8 CFU of *Candida albicans*. The fungi phagocytosed by macrophages (arrows) and neutrophils (arrowheads) are visible by PAS staining (magnification, ×100). (B and C) The proportions of macrophages (B) and neutrophils (C) phagocytosing *Candida albicans* in the peritoneal lavage fluids of wild-type (WT) mice and GATA-3-overexpressing (GATA) mice 3 days (Day 3) and 7 days (Day 7) after intraperitoneal inoculation of 1×10^8 CFU of *Candida albicans*. Experiments were performed in duplicate with five mice in each group. *, significantly different between wild-type mice and GATA-3-overexpressing mice ($P < 0.05$).

respectively, are the members of the CXC chemokine family that are the most critical for neutrophil recruitment to a site of infection (14). In the present study, consistently, the recruitment of macrophages into the peritoneal cavity, at the site of *Candida* infection, and the induction of MCP-1, KC, and MIP-2 in these cells were diminished in *GATA-3-tg* mice. Furthermore, administration of IFN-γ to *GATA-3-tg* mice increased the number of peritoneal macrophages. Thus, overexpression of GATA-3 may reduce macrophage antifungal activity by reducing the production of IFN-γ in response to *Candida* infection.

TNF-α is another Th1 cytokine produced by a variety of cells. It has been demonstrated that the administration of exogenous TNF-α enhances host resistance against systemic *Candida* infection, although TNF-α did not demonstrate a direct anticandidal effect *in vitro* (18). Endogenously produced TNF-α was also shown to have a beneficial effect in the host defense against *Candida* infection, since treatment of mice with anti-TNF-α antibody resulted in higher colony formation of *C. albicans* in the kidney and spleen early in the infection (18). The present finding that the expression of TNF-α was significantly lower in the spleens of *Candida*-susceptible *GATA-3-tg* mice than in those of WT mice is consistent with these previous findings.

To generate *GATA-3-tg* mice, we inserted a full-length murine GATA-3 cDNA into a VA CD2 transgene cassette (36). The VA vector has been reported to directly express the inserted cDNA in all single-positive mature T cells of transgenic mice (40). Since GATA-3 is a T-cell-specific transcription factor, transgenic mice are thought to be adequate for use in evaluating T-cell-mediated regulation of *Candida* infection. In the present study, intracellular cytokine analysis revealed that the suppression of IFN-γ production in *GATA-3-tg* mice occurred in CD4-positive T cells. These findings suggest that the overexpressed *GATA-3* gene actually acts on CD4-positive T cells in the present model.

Coordination between innate immunity and adaptive immunity is critical for host defense against fungal infections (4, 20). A variety of cells, including macrophages, neutrophils, natural killer cells, and natural killer T (NKT) cells, may participate in the nonspecific clearance of fungi as innate immune cells. On the other hand, Th1 cells and IFN-γ are clearly required for the expression of adaptive anticandidal responses (5, 26, 27). In the present analysis of peritoneal lavage fluids, macrophages, neutrophils, and NKT cells were predominant 1 day to 3 days following *Candida* inoculation (data not shown). On the other hand, CD4-positive T cells were predominant 5 days after *Candida* inoculation. These results indicate that adaptive immunity becomes predominant 5 days after the inoculation. In the present study, we

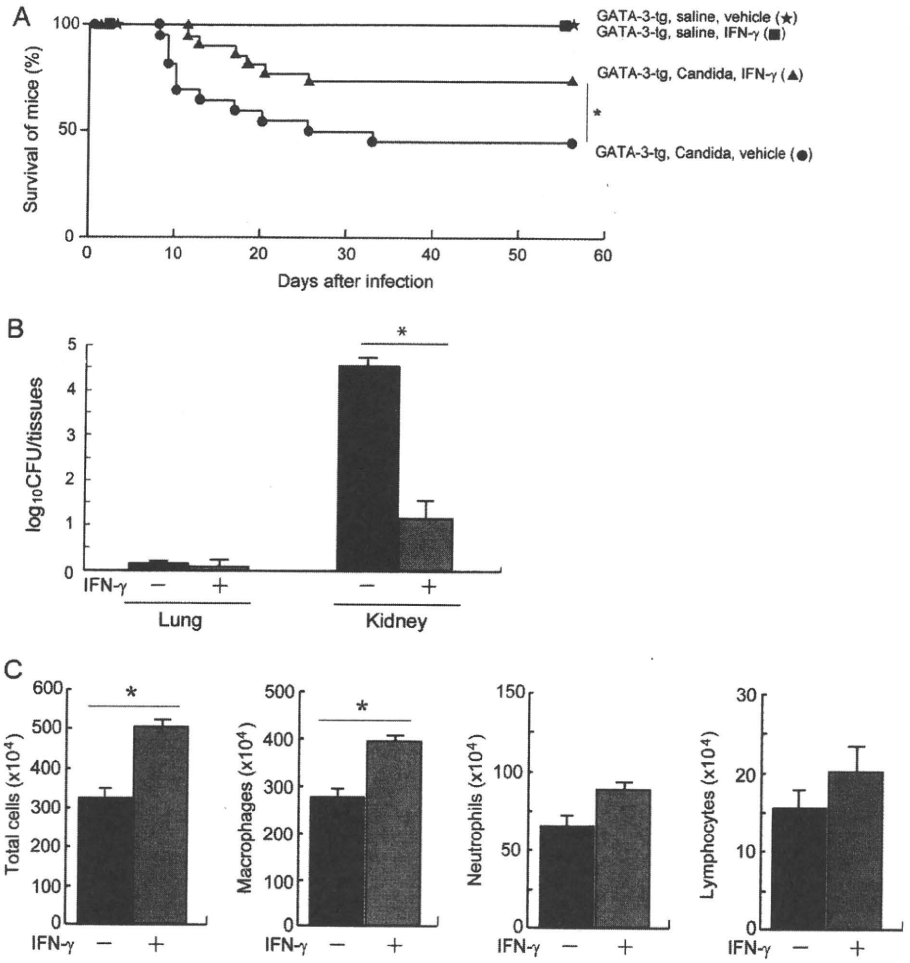

FIG. 7. Effects of gamma interferon supplementation on systemic *Candida* infection. (A) Survival of GATA-3-overexpressing mice treated with 8×10^6 U of gamma interferon (GATA-3-tg, Candida, IFN-γ) (triangles) or with vehicle (GATA-3-tg, Candida, vehicle) (circles) after intraperitoneal inoculation of 1×10^8 CFU of *Candida albicans*. The survival of GATA-3-overexpressing mice after intraperitoneal inoculation of saline was also evaluated with (squares) or without (stars) treatment with gamma interferon. $n = 20$ in each group. *, significantly different between the *GATA-3-tg–Candida*–IFN-γ group and *GATA-3-tg–Candida*–vehicle group ($P < 0.05$). (B) Outgrowth of *Candida albicans* in the lungs and kidneys of GATA-3-overexpressing mice treated with 8×10^6 U of IFN-γ (gray bars) or with vehicle (black bars) 56 days after *Candida albicans* inoculation. The results were expressed as $\log_{10}$ CFU per organ. Experiments were performed in duplicate with five mice in each group. *, significantly different between mice treated with IFN-γ and those treated with vehicle ($P < 0.05$). (C) The number of total cells, macrophages, neutrophils, and lymphocytes in the peritoneal lavage fluids of GATA-3-overexpressing mice treated with 8×10^6 U of IFN-γ (gray bars) or with vehicle (black bars) 56 days after *Candida albicans* inoculation. Experiments were performed in duplicate with five mice in each group. *, significantly different between mice treated with IFN-γ and with vehicle ($P < 0.05$).

consistently observed that *GATA-3-tg* mice had already begun to die at 5 days after *Candida* inoculation.

In conclusion, we demonstrated that mice overexpressing GATA-3 are highly susceptible to systemic *Candida* infection by both an intraperitoneal and an intravenous route. Overexpression of GATA-3 reduces IFN-γ production in CXC3-positive Th1 cells in response to *Candida* infection. IFN-γ insufficiency may impair macrophage anticandidal activity and thereby enhance the susceptibility to systemic *Candida* infection. We demonstrate here that GATA-3 is an important host factor in the regulation of susceptibility to *Candida* infection and that the determination of GATA-3 activation, as well as IFN-γ expression, in Th cells might serve as a useful clinical marker for predicting the severity of *Candida* infection.

ACKNOWLEDGMENT

This work was supported by a Grant-in-Aid for Scientific Research (C) in Japan from the Society for the Promotion of Science.

REFERENCES

1. **Abbas, A. K., K. M. Murphy, and A. Sher.** 1996. Functional diversity of helper T lymphocytes. Nature **383:**787–793.
2. **Antachopoulos, C., T. J. Walsh, and E. Roilides.** 2007. Fungal infection in primary immunodeficiencies. Eur. J. Pediatr. **166:**1099–1117.
3. **Ashman, R. B., and J. M. Papadimitriou.** 1995. Production and function of cytokines in natural and acquired immunity to Candida albicans infection. Microbiol. Rev. **59:**646–672.

4. **Ashman, R. B., C. S. Farah, S. Wanasaengsakul, Y. Hu, G. Pang, and R. L. Clancy.** 2004. Innate versus adaptive immunity in Candida albicans infection. Immunol. Cell Biol. **82:**196–204.
5. **Cenci, E., A. Mencacci, G. Del Sero, C. Fe d'Ostiani, P. Mosci, M. Kopf, and L. Romani.** 1998. IFN-γ is required for IL-12 responsiveness in mice with Candida albicans infection. J. Immunol. **161:**3543–3550.
6. **Chessler, A. D., M. Unnikrishnan, A. K. Bei, J. P. Daily, and B. A. Burleigh.** 2009. Trypanosoma cruzi triggers an early type I IFN response in vivo at the site of intradermal infection. J. Immunol. **182:**2288–2296.
7. **Dimopoulos, G., A. Karabinis, G. Samonis, and M. E. Falagas.** 2007. Candidemia in immunocompromised and immunocompetent critically ill patients: a prospective comparative study. Eur. J. Clin. Microbiol. Infect. Dis. **26:**377–384.
8. **Ferber, I. A., H. J. Lee, F. Zonin, V. Heath, A. Mui, N. Arai, and A. O'Garra.** 1999. GATA-3 significantly downregulates IFN-γ production from developing Th1 cells in addition to inducing IL-4 and IL-5 levels. Clin. Immunol. **91:**134–144.
9. **Gozalbo, D., and M. L. Gil.** 2009. IFN-gamma in Candida albicans infections. Front. Biosci. **14:**1970–1978.
10. **Ho, I. C., and L. H. Glimcher.** 2002. Transcription: tantalizing time for T cells. Cell **109:**S109–S120.
11. **Ho, I. C., T. S. Tai, and S. Y. Pai.** 2009. GATA3 and the T-cell lineage: essential functions before and after T-helper-2-cell differentiation. Nat. Rev. Immunol. **9:**125–135.
12. **Kaminuma, O., F. Kitamura, N. Kitamura, M. Miyagishi, K. Taira, K. Yamamoto, O. Miura, and S. Miyatake.** 2004. GATA-3 suppresses IFN-γ promoter activity independently of binding to cis-regulatory element. FEBS Lett. **570:**63–68.
13. **Kaposzta, R., P. Tree, L. Marodi, and S. Gordon.** 1998. Characteristic of invasive candidiasis in gamma interferon- and interleukin-4-deficient mice: role of macrophages in host defense against Candida albicans. Infect. Immun. **66:**1708–1717.
14. **Kobayashi, Y.** 2008. The role of chemokines in neutrophil biology. Front. Biosci. **13:**2400–2407.
15. **Lee, G. R., P. E. Field, and R. A. Flavell.** 2001. Regulation of IL-4 gene expression by distal regulatory elements and GATA-3 at the chromatin level. Immunity **14:**447–459.
16. **Liblau, R. S., S. M. Singer, and H. O. McDevitt.** 1995. Th1 and Th2 CD4+ T cells in the pathogenesis of organ-specific autoimmune diseases. Immunol. Today **16:**34–38.
17. **Liew, F. Y., X. Q. Wei, and L. Proudfoot.** 1997. Cytokines and nitric oxide as effector molecules against parasitic infections. Philos. Trans. R. Soc. Lond. B Biol. Sci. **352:**1311–1315.
18. **Louie, A., A. L. Baltch, R. P. Smith, M. A. Franke, W. J. Ritz, J. K. Singh, and M. A. Gordon.** 1994. Tumor necrosis factor alpha has a protective role in a murine model of systemic candidiasis. Infect. Immun. **62:**2761–2772.
19. **Mencacci, A., E. Cenci, G. Del Sero, C. Fe d'Ostiani, C. Montagnoli, and L. Romani.** 1999. Innate and adaptive immunity to Candida albicans: a new view of an old paradigm. Rev. Iberoam. Micol. **16:**4–7.
20. **Mencacci, A., E. Cenci, F. Bistoni, G. Del Sero, A. Bacci, C. Montagnoli, C. Fe d'Ostiani, and L. Romani.** 1998. Specific and non-specific immunity to Candida albicans: a lesson from genetically modified animals. Res. Immunol. **149:**352–361.
21. **Murphy, E., K. Shibuya, N. Hosken, P. Openshaw, V. Maino, K. Davis, K. Murphy, and A. O'Garra.** 1996. Reversibility of T helper 1 and 2 populations is lost after long term stimulation. J. Exp. Med. **183:**901–913.
22. **Ouyang, W., S. H. Ranganath, K. Weindel, D. Bhattacharya, T. L. Murphy, W. C. Sha, and K. M. Murph.** 1998. Inhibition of Th1 development mediated by GATA-3 through an IL-4-independent mechanism. Immunity **9:**745–755.
23. **Pai, S. Y., M. L. Truitt, and I. C. Ho.** 2004. GATA-3 deficiency abrogates the development and maintenance of T helper type 2 cells. Proc. Natl. Acad. Sci. U. S. A. **101:**1993–1998.
24. **Ranganath, S., W. Ouyang, D. Bhattarcharya, W. C. Sha, A. Grupe, G. Peltz, and K. M. Murphy.** 1998. GATA-3-dependent enhancer activity in IL-4 gene regulation. J. Immunol. **161:**3822–3826.
25. **Rangel-Frausto, M. S., T. Wiblin, H. M. Blumberg, L. Saiman, J. Patterson, M. Rinaldi, M. Pfaller, J. E. Edwards, Jr., W. Jarvis, J. Dawson, and R. P. Wenzel.** 1999. National epidemiology of mycoses survey (NEMIS): variations in rates of bloodstream infections due to Candida species in seven surgical intensive care units and six neonatal intensive care units. Clin. Infect. Dis. **29:**253–258.
26. **Romani, L., A. Mencacci, E. Cenci, R. Spaccapelo, P. Mosci, P. Puccetti, and F. Bistoni.** 1993. $CD4^+$ subset expression in murine candidiasis. Th responses correlate directly with genetically determined susceptibility or vaccine-induced resistance. J. Immunol. **150:**925–931.
27. **Romani, L.** 1997. The T cell responses to fungi. Curr. Opin. Immunol. **9:**484–490.
28. **Romani, L.** 1999. Immunity to *Candida albicans*: Th1, Th2 cells and beyond. Curr. Opin. Microbiol. **2:**363–367.
29. **Romani, L.** 2000. Innate and adaptive immunity in *Candida albicans* infections and saprophytism. J. Leukoc. Biol. **68:**175–179.
30. **Rudmann, D. G., A. M. Preston, M. W. Moore, and J. M. Beck.** 1998. Susceptibility to Pneumocystis carinii in mice is dependent on simultaneous deletion of IFN-gamma and type 1 and 2 TNF receptor genes. J. Immunol. **161:**360–366.
31. **Serbina, N. V., T. Jia, T. M. Hohl, and E. G. Pamer.** 2008. Monocyte-mediated defense against microbial pathogens. Annu. Rev. Immunol. **26:** 421–452.
32. **Subauste, C. S., and J. S. Remington.** 1991. Role of gamma interferon in Toxoplasma gondii infection. Eur. J. Clin. Microbiol. Infect. Dis. **10:**58–67.
33. **Takemoto, N., Y. Kamogawa, H. J. Lee, H. Kuruta, K. Arai, A. O'Garra, N. Arai, and S. Miyataka.** 2000. Chromatin remodeling at the IL4/IL13 intergenic regulatory region for Th2-specific cytokine gene cluster. J. Immunol. **165:**6687–6691.
34. **Usui, T., R. Nishikomori, A. Kitani, and W. Strober.** 2003. GATA-3 suppresses Th1 development by downregulation of Stat4 and not through effects on IL-12Rbeta2 chain or T-bet. Immunity **18:**415–428.
35. **Wisplinghoff, H., T. Bischoff, S. M. Tallent, H. Seifert, R. P. Wenzel, and M. B. Edmond.** 2004. Nosocomial bloodstream infections in US hospitals: analysis of 24,179 cases from a prospective nationwide surveillance study. Clin. Infect. Dis. **39:**309–317.
36. **Yoh, K., K. Shibuya, N. Morito, T. Nakano, K. Ishizaki, H. Shimohata, M. Nose, S. Izui, A. Shibuya, A. Koyama, J. D. Engel, M. Yamamoto, and S. Takahashi.** 2003. Transgenic overexpression of GATA-3 in T lymphocytes improved autoimmune glomerulonephritis in mice with a BXSB/Mpj-Yaa genetic background. J. Am. Soc. Nephrol. **14:**2494–2502.
37. **Zhang, D. H., L. Cohn, P. Ray, K. Bottomly, and A. Ray.** 1997. Transcription factor GATA-3 is differentially expressed in murine Th1 and Th2 cells and controls Th2-specific expression of the interleukin-5 gene. J. Biol. Chem. **272:**21597–21603.
38. **Zhang, D. H., L. Yang, and A. Ray.** 1998. Differential responsiveness of the IL-5 and IL-4 genes to transcription factor GATA-3. J. Immunol. **161:**3817–3821.
39. **Zheng, W. P., and R. A. Flavell.** 1997. The transcription factor GATA-3 is necessary and sufficient for Th2 cytokine gene expression in CD4 T cells. Cell **89:**587–596.
40. **Zhumabekov, T., P. Corbella, M. Tolaini, and D. Kioussis.** 1995. Improved version of a human CD2 minigene based vector for T cell-specific expression in transgenic mice. J. Immunol. Methods **185:**133–140.

Editor: G. S. Deepe, Jr.